Supporting Information

Immune Checkpoint Ligand-Bioengineered Schwann Cells as Antigen-Specific Therapy for Experimental Autoimmune Encephalomyelitis

Kin Man Au, Roland Tisch, and Andrew Z. Wang**

Materials and Methods

Materials. N-azidoacetylmannosamine tetraacylated (Ac_4ManNAz), dibenzocyclooctyne-functionalized oligoethylene glycol N-hydroxysuccinimide ester (DBCO-PEG13-NHS ester; 95%), and trans-cyclooctene-functionalized oligoethylene glycol N-hydroxysuccinimide ester (TCO-PEG4-NHS ester, ≥ 95%) were purchased from Click Chemistry Tools (Scottsdale, AZ). Leflunomide (Pharmaceutical Secondary Standard), water (BioReagent), acetonitrile (HPLC grade, ≥ 99%), dimethyl sulfoxide (anhydrous, ≥ 99.9%), poly(lactide-co-glycolide) (PLGA, ester terminated; M_w = 50 kDa – 70 kDa), and formaldehyde solution (4%, buffered, pH 6.9) were purchased from Sigma (St Louis, MO).

Poly(lactide-co-glycolide)-block-poly(ethylene glycol)-dibenzocyclooctyne endcap (DBCO-PEG-PLGA; M_w = (5 + 10) kDa = 15 kDa) was purchased from Nanosoft Polymers (Winston-Salem, NC). Poly(lactide)-block-poly(ethylene glycol)-methyletrazine endcap (MTZ-PEG-PLA; AI150; M_w = (16 + 5) kDa = 21 kDa), methoxy poly(ethylene glycol)-b-poly(D,L-lactic-co-glycolic) acid copolymer (mPEG-PLGA; AK10; M_w = (3 + 20) kDa = 23 kDa), and poly(lactide-co-glycolide)-Cyanine 5 (Cy5-PLGA; AV034, M_w = 30 – 55 kDa) were purchased from Akina, Inc (West Lafayete, IN).

Alexa Fluor 488 NHS ester, Texas Red-X NHS ester (mixture of isomers), Zeba Spin 7K MWCO Desalting Columns (Thermo Fisher), VivoTack 680 NIR fluorescent Imaging Agent (Perkin Elmer LLC), sulfo-cyanine 5 tetrazines (Lumiprobe), Dynabeads™ Mouse T-Activator

CD3/CD28 T cells Activation Beads (Gibco), EasySep™ Mouse $CD4^+$ T Cell Isolation Kit (STEMCELL Technologies), EasySep™ Mouse $CD8^+$ T Cell Isolation Kit (STEMCELL Technologies), recombinant mouse IL-2 (R&D Systems) and CellTiter96® AQueous MTS Powder (Promega) were purchased from Fisher Scientific (Hampton, NH). Unless specified, all antibodies for flow cytometry studies were purchased from Fisher Scientific (Hampton, NH). Recombinant mouse PD-L1 FcIg fusion protein (PD-L1 FcIg; molecular weight = 102 kDa; PR00112-1.9), and recombinant mouse CD86 FcIg fusion protein (CD86 FcIg; molecular weight = 103 kDa; PR00226-1.9) were purchased from Absolute Antibody NA (Boston, MA). Both fusion proteins were supplied in sterilized 1X PBS. The Mouse Interferon gamma ELISA Kit (ab100689) and mouse IL-17A ELISA Kit (ab199081) were purchased from Abcam PLC (Cambridge, MA).

Anti-CD25 antibody (InVivoMAb, clone: PC-61.5.3, catalog number: BE0012) Was purchased from BioXCell (Lebanon, NH).

EAE induction kits (MOG_{35-55}/CFA emulsion (contain 1 mg/mL of MOG_{35-55}) and a tailor-made $PLP_{178-191}$/CFA emulsion (contain 0.25 mg/mL of $PLP_{178-191}$)[34]) were purchased from Hooke Laboratories, Inc (Lawrence, MA).

Methods

Functionalization of PD-L1 FcIg and CD86 FcIg fusion proteins

PD-L1 FcIg and CD86 FcIg fusion proteins were functionalized *via* amine-NHS ester coupling chemistry [19, 43]. DBCO-functionalized fusion proteins were functionalized *via* amine-NHS ester coupling reaction between the fusion protein and DBCO-PEG13-NHS ester at pH 8.0 (20°C) for 2 h. The target degrees of functionalization were 15, 30, and 45 for the pilot functionalization study, and a target degree of 45 (leading to an actual degree of function of approximately 9) was used for the subsequent functionalization study. The functionalized fusion proteins were purified by Zeba Spin 7K MWCO desalting column according to the

manufacturer's protocol. The concentrations and degrees of the DBCO incorporation of different purified DBCO-conjugated fusion proteins were determined spectroscopically using an absorption coefficient of DBCO at 310 nm ($\varepsilon_{DBCO,310nm}$) = 12,000 M^{-1} L cm^{-1}, an absorption coefficient of mouse immunoglobulin at 280 nm (ε_{280nm}) = 1.26 mg^{-1} mL cm^{-1} (for PD-L1 FcIg)/1.34 mg^{-1} mL cm^{-1} (for CD86 FcIg), and a DBCO correction factor at 280 nm ($CF_{DBCO,280nm}$) = 1.089 according to the manufacturer's instructions. The TCO-functionalized fusion proteins were prepared via the same method with a target degree of functionalization of 45. A488-labeled DBCO-functionalized PD-L1 FcIg and Texas Red (TexRed)-labeled DBCO-functionalized CD86 FcIg were prepared *via* the same method with a target degree of functionalization of 45 and 5 respectively. The concentrations of the purified dye-labeled fusion proteins were quantified *via* the Pierce BCA Protein assay kit (Thermo Fisher). The number of conjugated dye molecules belonging to the known concentration of fusion protein was calculated from the corresponding UV-visible absorption spectrum that used an absorption coefficient of 71,000 M^{-1} L cm^{-1} (at 495 nm) for the conjugated A488 dye or 80,000 M^{-1} L cm^{-1} (at 595 nm) for the conjugated Texas Red.

Preparation of drug-free/LEF-encapsulated DBCO/MTZ-functionalized PEG-PLGA NPs

Drug-free DBCO/MTZ-functionalized PEG-PLGA NPs (DBCO/MTZ NPs) were prepared *via* the nanoprecipitation method [43]. For the preparation of 30 mg of DBCO/MTZ NPs, 9 mg of DBCO-PEG-PLGA, 9 mg of MTZ-PEG-PLA, 12 mg of mPEG-PLGA, and 6 mg PLGA (consider as payload) were first dissolved into 3 mL of acetonitrile. The polymer blend was then added slowly (1 mL/min) to 12 mL of deionized water under constant stirring (1,000 rpm). The mixture was stirred under reduced pressure for 2 h before purifying it 3 times *via* Amicron Ultra ultrafiltration membrane filter (MWCO 100,000) as per the manufacturer's protocol. Cy5-labeled DBCO/MTZ NPs were prepared *via* the same method, except using Cy5-labeled PLGA instead of non-functionalized PLGA.

LEF-encapsulated DBCO/MTZ-functionalized PEG-PLGA NPs (DBCO/MTZ LEF NPs) were prepared *via* the same nanoprecipitation method with the addition of 7.25 wt/wt% of LEF in the polymer blend for preparing the NPs. The LEF loading in the purified NPs was quantified *via* fluorescence spectroscopy (excitation wavelength = 280 ± 20 nm; emission wavelength = 410 ± 20 nm), as previously reported. An *in vitro* drug release study was performed *via* Slide-A-Lyzer MINI Dialysis Devices (20K MWCO, Thermo Fisher) in the presence of a large excess of 1X PBS at 37°C (in the dark). Unreleased LEF in the NPs was quantified *via* fluorescence spectroscopy [21].

Drug-free and LEF-encapsulated NPs suspended in 1X PBS were characterized by transmission electron microscopy (TEM) and the dynamic light scattering method. TEM images were recorded in a JEOL 1230 transmission electron microscope in Microscopy Services Laboratory (MSL) at the UNC School of Medicine. Before the imaging study, carbon-coated copper grids were glow discharged, and the samples were negatively stained with tungsten acetate (pH 7). The intensity-average diameter of both purified NPs (suspended in 1X PBS) was determined by a Zetasizer Nano ZSP Dynamic Light Scattering Instrument (Malvern).

***In vitro* studies**

Cell lines. Mouse Schwann cells (MSCs, catalog number: T0295), isolated from the C57BL/6 mice, were purchased from Applied Biological Materials Inc. (ABM Inc.; Richmond, BC). MSCs were cultured in G422 Applied Cell Extracellular Matrix-coated cell culture flashes (catalog number: G422; ABM Inc.) in Prigow III Medium (catalog number TM003; ABM Inc.). This was supplemented with 10% FBS (Sigma) according to the manufacturer's protocol.

Mouse oligodendrocytes (MOLs, catalog number: 11004-02), isolated from the C57BL/6 mice, were purchased from Celprogen, Inc. (San Pedro, CA). MOLs were cultured in G422 Applied Cell Extracellular Matrix-coated cell culture flashes (catalog number: G422; ABM Inc.) in mouse oligodendrocytes primary cell culture complete medium with serum (catalog number: M11004-25; Celprogen, Inc) according to manufacturer's protocol.

The MOG and PLP expressions of MSCs and MOLs were separately quantified *via* the FACS method after stained with anti-myelin oligodendrocyte glycoprotein antibody (catalog number: A3992, ABclonal) and anti-PLP1 polyclonal antibody (catalog number: A20009, Abclonal). Both non-labeled rabbit antibodies were visualized by A488-labeled anti-rabbit IgG (H+L) Cross-Adsorbed Antibody (catalog number: A-11008, Invitrogen). MIN-6 cells (ATCC), established by the insulinoma cell line and isolated from C57BL/6 mice, were used as a negative control for both antibodies.

MOG-specific $CD4^+$ T cells (2D2 cells) were isolated from 2D2 mice as previously reported[24]. Briefly, $CD4^+$ T cells were isolated from the splenocytes of 2D2 mice (C57BL/6-Tg (Tcra2D2, Tcrb2D2) 1Kuch/J; female, 7–8 weeks old, stock number: 006912, The Jackson Laboratory) using the immunomagnetic negative selection method *via* an EasySep™ Mouse $CD4^+$ T Cell Isolation Kit (STEMCELL Technologies), as per the given manufacturer's rules.

$CD8^+$ T cells were isolated from the splenocytes of wild-type C57BL/6 mice (female, about 8 weeks old; Charles River Laboratories) using the immunomagnetic negative selection method *via* an EasySep™ Mouse $CD8^+$ T Cell Isolation Kit (STEMCELL Technologies). After isolation, $CD8^+$ T cells were seeded into a 24-well plate at a density of 2×10^6 cells per well with a 2 mL medium. T cells were expanded with anti-CD3/antiCD28 antibody-conjugated beads (Life Technologies, Grand Island, NY) at a bead-to-cells ratio of 2:1 in the presence of 2,000 IU/mL of recombinant mouse IL-2 (R&D Systems, Minneapolis, MN) in complete RPMI 1640 (Gibco) medium supplemented with 10% v/v fetal bovine serum (FBS, Seradigm), 2mM GlutaMAX Supplement (Gibco), and antibiotic-antimycotic (Anti-Anti; 100 units of penicillin, 100 μg/mL of streptomycin, and 0.25 μg/mL of amphotericin B; Gibco) for 48 h before further studies.

***In vitro* toxicity of Ac_4ManNAz and LEF, and viabilities of functionalized MSCs**

In vitro toxicities of Ac_4ManNAz and LEF against MSCs, and the viabilities of functionalized MSCs were quantified by MTS assay. Briefly, treated/functionalized cells were cultured in

complete media for 4 days. The phenol-red media was replaced by phenol red-free DMEM (supplemented with 10% FBS) before quantifying the viabilities *via* MTS assay according to the manufacturer's protocol. The MSCs were seeded at a density of 2×10^4 cells per well in a 96-well plate.

Preparation of azide-modified MSCs

Azide-modified MSCs were generated by the culture in a complete growth medium containing 50 μM of Ac_4ManNAz for 4 days. The Ac_4ManNAz-containing culture medium was refreshed every 48 h. Azide-modified cells were detached *via* TrypLE™ Express Enzyme (Gibco) according to the manufacturer's protocol for subsequent studies. The Ac_4ManNAz-containing culture medium was refreshed every 48 h.

Functionalization of azide-modified MSCs with PD-L1 FcIg and CD86 FcIg

Two bioconjugation methods were investigated to functionalize MSCs.

In the direct bioconjugation method, DBCO-functionalized PD-L1 FcIg and/or CD86 FcIg were conjugated to azide-modified MSCs *via* SPAAC at 37°C for 1 h. The target degree of functionalization was 5 μg fusion protein per one million cells. The bioconjugation was carried out at 20 million cells per mL. Functionalized MSCs were purified *via* centrifugation (300 g, 3 – 4 min, 3 times) and resuspended in complete media for subsequent *in vitro* studies or 1X PBS for subsequent in vivo studies.

In the NP-pre-anchoring method, DBCO/MTZ NPs were first conjugated to the azide-modified MSCs *via* SPAAC at 37°C for 1 h. The target degree of functionalization was 500 μg of DBCO/MTZ NPs per one million cells (cell concentration: 20 million cells per mL). NP-functionalized MSCs were purified *via* centrifugation (300 g, 3 – 4 min, 3 times). TCO-functionalized PD-L1 FcIg and/or CD86 FcIg were added to the NP-functionalized MSCs *via* IEDDA at 37°C for 1h. As with the first bioconjugation method, the target degree of functionalization was 5 μg fusion protein(s) per million cells. Functionalized MSCs were purified *via* centrifugation (300 g, 3 – 4 min, 3 times) and resuspended in complete media for

subsequent *in vitro* studies or 1X PBS for subsequent *in vivo* studies. For selected *in vivo* experimental groups, functionalized MSCs were subjected to 100 Gy X-ray irradiation (*via* a RS2000 Biological Irradiator, operated at 160 kV and 24 mA) before administrated to the EAE mice.

The viabilities of functionalized MSCs cells were quantified by MTS assay at 4 days post-functionalization. The sizes of unmodified and functionalized MSCs were determined by using an ORFLO Moxi Z Mini Automated Cell Counter.

The amount(s) of conjugated fusion protein(s) were quantified *via* fluorescence spectroscopy using A488-labeled PD-L1 FcIg (excitation wavelength = 480 ± 20 nm; emission wavelength = 525 ± 20 nm) or Texas Red-labeled CD86 FcIg (excitation wavelength = 550 ± 20 nm; emission wavelength = 640 ± 20 nm) for the bioconjugation. The amounts of MSC- -conjugated NPs were quantified *via* fluorescence spectroscopic method using Cy5-labeled DBCO/MTZ NPs (excitation wavelength = 640 ± 20 nm; emission wavelength = 780 ± 20 nm) for the bioconjugation. Functionalized dye-labeled cells were exchanged into PBS before fluorescence spectroscopic measurements. The detachment of the dye-labeled fusion proteins and NPs were monitored *via* fluorescence spectroscopy.

A time-dependent FACS study was used to quantify the PD-L1 and CD86 expressions of unmodified and functionalized MSCs. At a desired point of time, cells were detached and blocked with rat anti-mouse CD16/CD32 (mouse BD Fc Block; BD Bioscience) before being stained with PE-labeled anti-mouse PD-L1 antibody (clone: MIH5, catalog number: 12-5982-82; Invitrogen) and FITC-labeled anti-mouse CD86 antibody (clone: GL1; catalog number: 11-0862-82; Invitrogen). Stained cells were then fixed with 4% paraformaldehyde (4% PFA; Sigma) and kept in dark at 4°C before further FACS study. The PD-L1 and CD86 expressions of different functionalized MSCs were further evaluated by CLSM method after stained with PE-labeled anti-mouse PD-L1 antibody (clone: MIH5, catalog number: 12-5982-82;

Invitrogen) and FITC-labeled anti-mouse CD86 antibody (clone: GL1; catalog number: 11-0862-82; Invitrogen).

For the CLSM study, MSCs were seeded in G422 Applied Cell Extracellular Matrix-coated microscope coverslips (1 cm diameter) in a 12-well plate. Cells were cultured with 50 μM of Ac_4ManNAz for 4 days, before functionalized with DBCO-functionalized PD-L1 FcIg and/or CD86 FcIg, or DBCO/MTZ NPs followed by TCO-functionalized PD-L1 FcIg and CD86 FcIg. Next, the MSCs were stained with PE-labeled anti-PD-L1, and FITC-labeled anti-CD86 were recorded in a Zeiss LSM 710 Spectral Confocal Laser Scanning Microscope in the MSL at the UNC School of Medicine.

For field-emission scanning electron microscopy study, MSCs were seeded in G422 Applied Cell Extracellular Matrix-coated microscope coverslips (1 cm diameter) in a 12-well plate. Cells were cultured with 50 μM of Ac_4ManNAz for 4 days, before functionalized with DBCO/MTZ NPs, followed by TCO-functionalized PD-L1 FcIg and CD86 FcIg. After functionalization, MSCs were then washed with 1X PBS containing 10 mM magnesium chloride three times before fixing with 10% neutral-buffered formalin. The FE-SEM images were recorded using a Zeiss Supra 25 FESEM microscope in the MSL at the UNC School of Medicine.

Myelin-specific CD4 T cell *in vitro* activation

Mouse IFN-γ and mouse IL-17A secreted from the activated myelin-specific 2D2 cells were quantified by ELISA assays as previously reported [24]. The PD-1 and CTLA-4 expressions of myelin-specific 2D2 cells were quantified *via* the FACS method. Briefly, 2D2 cells (effector cells (E)) were cultured with different non-functionalized and functionalized MSCs and MOLs (target cells (T): 5×10^4 cells per well in a 6-well plate that were seeded for 4 h before co-cultured with the 2D2 cells) at an E:T ratio of 10:1 for 48 h. The cell culture media (contain mainly the 2D2 cells) were preserved. 2D2 cells were collected from the cultured media *via* centrifugation at 1,000g for 10 min. The moue IFN-γ and mouse IL-17A concentrations in the supernatants

were quantified *via* mouse IFN-γ ELISA kit (ab100689; Abcam, Cambridge, MA) and mouse IL-17A ELISA kit (ab199081; Abcam, Cambridge, MA), according to manufacturer's instructions. The PD-1 and CTLA-4 expressions of the isolated 2D2 cells were quantified *via* FACS method after stained with A488-labeled anti-mouse PD-1 antibody (clone: MIH4, catalog number: 53-9969-42, Invitrogen), PE-labeled anti-mouse CTLA-4 antibody (clone: UC10-4B9, catalog number: 50-106-52, Invitrogen), and eFluor 660-labeled anti-mouse CD3 antibody (clone: 17A2, catalog number: 50-0032-82, Invitrogen)[24]. Stained cells were fixed with 4% paraformaldehyde (4% PFA; Sigma) and kept in dark at 4°C before further FACS study.

The differentiation of naïve 2D2 cells into $IL10^+$ $FoxP3^+$ T_{reg} cells was quantified by FACS as previously reported[24]. The 2D2 cells were briefly cultured with different non-functionalized and functionalized MSCs (5×10^4 cells per well in a 6-well plate that seeded for 4 h before co-cultured with the 2D2 cells) at an E:T ratio of 10:1 for 72 h. 2D2 cells were collected from the cultured media *via* centrifugation at 1,000g for 10 min. The isolated cells were first stained with eFluor 660-labeled anti-mouse CD3 antibody (clone: 17A2, catalog number: 50-0032-82, Invitrogen). They were then fixed with 4% PFA before permeabilization using the intracellular staining permeabilization wash buffer (Biolegend). Further, they were stained with A488-labeled anti-mouse FoxP3 antibody (clone: MF23, catalog number: 560403, BD Bioscience) and PE-labeled anti-mouse IL10 antibody (clone: JES5-16E3, catalog number: 561060, BD Bioscience) for FACS study.

Quantification of antigen-non-specific cytotoxic T cell inhabitation

The abilities for the functionalized MSCs to inhibit cytotoxic T cell activation were quantified by CellTrace CFSE Cell Proliferation assay (Thermo Fisher). Briefly, the CFSE-labeled expanded $CD8^+$ T cells (isolated from wide-type C57BL/6 mice) were cultured with seeded unmodified/ functionalized MSCs at an E:T ratio of 10:1 for 48 h in the presence of 1 molar

equivalent (vs $CD8^+$ T cells) of Dynabeads™ Mouse T-Activator CD3/CD28 T cells Activation Beads (Gibco) [44]. The proliferation of CFSE-labeled $CD8^+$ T cells was quantified *via* FACS.

***In Vivo* Studies**

Animals were maintained in the Division of Comparative Medicine (an AAALAC-accredited experimental animal facility) under sterile environments at the University of North Carolina. All procedures involving the experimental animals were performed following the protocols that the University of North Carolina Institutional Animal Care and Use Committee has approved, and they conformed with the Guide for the Care and Use of Laboratory Animals (NIH publication no. 86-23, revised 1985). Mice were randomized and grouped on arrival. Grouped mice were housed in the animal facility for at least 7 days before EAE induction.

***In vivo* toxicity of i.v. administered unmodified and PD-L1 FcIg/CD96 FcIg NP-functionalized MSCs**

The long-term *in vivo* toxicities of the i.v. administered MSCs and PD-L1 FcIg/CD86 FcIg NP-functionalized MSCs (2 million cells/mouse) were evaluated in healthy C56BL\6 mice (15 weeks old, female, Charles River Laboratories). The mice's body weight was monitored weekly after the administration. 5 weeks later, the mice were euthanized *via* an overdose of ketamine. Full blood and key organs were preserved for clinical chemistry and histopathological studies in the Animal Histopathology and Lab Medicine Core at the UNC School of Medicine.

EAE induction and clinical evaluation

EAE was induced in wide-type C57BL/6 mice (female, 15–16 weeks old) through an active immunization method. For the induction of MOG_{35-55} EAE in C56BL/6 mice, 200 µl of MOG_{35-55}/CFA emulsion (containing 200 µg of MOG_{35-55} and about 0.8 mg of heat-killed mycobacterium tuberculosis; Hooke Laboratories, Lawrence, MA) was subcutaneously administrated to each C56BL\6 mouse. According to manufacturer's guidelines (https://hookelabs.com/protocols/eaeAI_C57BL6.html) and other representative EAE studies,[45] we randomized, grouped and ear-tagged the mice at least 1 week before the EAE

induction to prevent stress affect EAE progression. For the induction of $PLP_{178-191}$ EAE in C56BL/6 mice, 200 µl of $PLP_{178-191}$/CFA emulsion (containing 50 µg of $PLP_{178-191}$ and about 0.8 mg of heat-killed mycobacterium tuberculosis; Hooke Laboratories, Lawrence, MA) was subcutaneously given to each C56BL/6 mouse. No pertussis toxin was administered for the EAE induction. The body weight and clinical signs were monitor daily post-immunization. The EAE clinical signs were scored on 0 to 5.0 scale as follows: score 0: normal mouse; score 0.5: partial tail paresis; score 1.0: complete tail paresis; score 1.5: limp tail and hind leg inhibition; score 2.0: limp tail and weakness of hind legs; score 2.5: limp tail and no movement in one leg; score 3.0: complete hind limb paralysis; score 4.0: hind limb paralysis and forelimb weakness; score 5.0: moribund. The paralyzed mice were afforded easier access to food and water. Unless specified, MSCs were administrated *via* tail vein i.v. injection. For the prophylactic study, unmodified MSCs or functionalized MSCs (2 million cells per mouse) were administered 1-day post-immunization. For the therapeutic treatment study, unmodified MSCs or functionalized MSC (2 million cells per mouse) were administered on day 17 or 18 p.i., when the EAE-inflicted mice showed severe EAE symptoms (EAE score ≈ 2.0). For the selected studies, a booster dose of functionalized MSCs was i.v. administered on day 28 or 35 p.i. In a selected *in vivo* study, functionalized MSCs were intramuscularly administrated to the tight muscles at the hind limb. Unless specified, mice were euthanized, and spinal columns were preserved on day 36 or 37 p.i. *via* full-body perfusion method for further histopathological studies. Preserved spinal columns were processed by the Animal Histopathology and Lab Medicine Core at the UNC School of Medicine for hematoxylin and eosin (H&E), Luxol fast blue (LFB), and anti-CD4 and anti-FoxP3 immunohistochemistry stains. H&E- and LFB-stained slides were imaged *via* a ScanScope AT2 (Leica Biosystems) pathology slide scanner. Spinal inflammation was quantified from representative H&E-stained sections[46]. Anti-CD4 and anti-FoxP3 immunofluorescence-stained slides were imaged *via* a ScanScope FL (Leica Biosystems) pathology slide scanner.

T_{reg} cell depletion study

T_{reg} cell depletion study was performed in MOG_{35-55} EAE-inflicted mice to demonstrate that the T_{reg} cells induced by the bioengineered MSCs play a key role in maintaining immunotolerance. The T_{reg} cells were depleted by an i.p. administration of 750 μg of anti-CD25 antibody (InVivoMAb, clone: PC-61.5.3, catalog number: BE0012; BioXCell), as previously reported. For the prophylactic study, the anti-CD25 antibody was administered on days 1, 3, and 5 p.i. (3×250 μg of anti-CD25)[36]. PD-L1 FcIg/CD86 FcIg NP-functionalized MSCs were i.v. administrated on day 2 p.i. For the therapeutic study, the anti-CD25 antibody was administered on days 17, 19, and 21 p.i. (3×250 μg of anti-CD25). PD-L1 FcIg/CD86 FcIg NP-functionalized MSCs were i.v. administrated on day 18 p.i., when the mice had an average clinical score of 2.0. Bodyweight and clinical signs were monitored daily after immunization. Control groups EAE-inflicted mice did not receive i.p. injections of anti-CD25 before and after the treatment with the functionalized MSCs.

***In vivo* biodistribution study of i.v. administered MSCs in MOG_{35-55} EAE-inflicted mice**

The biodistribution of i.v. administered MSCs was determined by the *ex vivo* NIR fluorescence imaging method. For the biodistribution study, non-functionalized or azide-functionalized MSCs were first labeled with VivoTag 680 (VT680) Fluorescent Dye (Perkin Elmer), according to the manufacturer's protocol. VT680-labeled azide-modified MSCs were functionalized *via* the same method as the non-labeled MSCs. For the prophylactic imaging groups, different VT680-labeled MSCs were i.v. administrated 1 day p.i. The mice were euthanized 48 h after the administration of MSCs, and the key organs were preserved for *ex vivo* imaging study in an AMI HT Optical Imaging System (excitation wavelength = 675 ± 25 nm, emission wavelength = 730 ± 25 nm, exposure time = 30 s, excitation power = 40%) in the Biomedical Research Imaging Center at the UNC School of Medicine. For the therapeutic imaging groups, different VT680-labeled MSCs were i.v. administrated 17 days p.i. The mice were euthanized 48 h after the administration of the labeled MSCs. Key organs were preserved for *ex vivo* imaging study

in an AMI HT Optical Imaging System (excitation wavelength = 675 ± 25 nm, emission wavelength = 730 ± 25 nm, exposure time = 30 s, excitation power = 40%) in the Biomedical Research Imaging Center at the UNC School of Medicine. The percentage of injected dose (% ID) of VT-680-labeled MSCs that was accumulated in each organ was calculated by comparing the fluorescence intensities of different standard VT680-labeled MSC samples.

***In vivo* mechanistic study**

A mechanistic study was performed on the MOG_{35-55} EAE-inflicted mice. For the prophylactic treatment groups, the mice received i.v. administration of unmodified/functionalized MSCs on day 2 p.i. The mice were euthanized on day 5 or 38 p.i., and spleens were preserved for further mechanistic study. On the other hand, the mice from the therapeutic treatment groups received i.v. administration of unmodified/functionalized MSCs on day 18 p.i. The treated mice were then euthanized on day 21 or 38 p.i., and spleens and spinal cords were preserved for further mechanistic study.

All the cell-based analyses were performed on single-cell suspensions of the spleen and spinal cord. For the isolation of splenocytes, the freshly preserved spleen was mashed through a cell strainer (70 μm; Fisher) in HBBS buffer. Erythrocytes were removed by ACK Lysis Buffer (Gibco) according to the manufacturer's protocol. The isolated splenocytes were first stained with T-Select I-Ab MOG35-55 Tetramer PB (Catalog number: TS0M704-1; MBL International, Woburn, MA). After the removal of the unbound tetramer, the cells were stained with Fixable Viability Stain 510 (catalog number: 564406; BD Bioscience), followed by A488-labeled anti-mouse CD4 antibody (clone: GK1.5; Invitrogen). The cells were then fixed with 4% PFA (Sigma) before permeabilization using the intracellular staining permeabilization wash buffer (Biolegend). They were then stained with DyLight 650 anti-mouse FoxP3 polyclonal antibody (catalog number: PA5-22773, Invitrogen), PE-Cyanine 7-labeled anti-mouse ROR-γ antibody (clone: B2D; catalog number: 25-6981-82, Invitrogen), and PE-Cyanine 5-labeled anti-mouse T-bet antibody (clone: 4B10; catalog: 15-5825-82) for FACS study via a Thermo Fisher Attune

NxT Analyzer or Intellicyt iQue Screener PLUS Analyzer in the Flow Cytometry Core Facility in the UNC School of Medicine.

The CNS-infiltrated lymphocytes were isolated from the freshly preserved spinal cord as previously reported. The isolated spinal cord was cut into small pieces and digested in a buffer solution that contained collagenase D (1 mg/mL; Roche) and DNase I (0.1 mg/mL, Roche) at 37°C for 20 min. The tissues were mashed through a cell strainer (70 μm; Fisher) to collect single cells. Lymphocytes (at the interface of between 37% and 70% Percoll gradient) were isolated using Percoll gradients (GE Healthcare) *via* the centrifugation method as previously reported. The isolated lymphocytes were divided into two halves. One half of the lymphocytes were first stained with Fixable Viability Stain 510 (catalog number: 564406; BD Bioscience), followed by A488-labeled anti-mouse CD8a antibody (clone: 53-6.7; catalog: 53-0081-82, Invitrogen). Cells were then fixed with 4% PFA (Sigma) before permeabilization using the intracellular staining permeabilization wash buffer (Biolegend), and this was followed by staining with PE-Cyanine 7 anti-mouse IFN-gamma antibody (clone: XMG1.2; catalog number: 25-7311-41, Invitrogen) for FACS study. For the other half of the isolated lymphocytes, cells were first stained with T-Select I-Ab MOG35-55 Tetramer PB (Catalog number: TS0M704-1; MBL International, Woburn, MA) according to the manufacturer's protocol. After the removal of the unbound tetramer, cells were stained with Fixable Viability Stain 510 (catalog number: 564406; BD Bioscience) and A488-labeled anti-mouse CD4 antibody (clone: GK1.5; Invitrogen). Similar to the previous steps, the cells were fixed with 4% PFA (Sigma) before permeabilization using an intracellular staining permeabilization wash buffer (Biolegend). Finally, they were stained with DyLight 650 anti-mouse FoxP3 polyclonal antibody (catalog number: PA5-22773, Invitrogen), PE-Cyanine 7 anti-mouse IFN-gamma antibody (clone: XMG1.2; catalog number: 25-7311-41, Invitrogen), and PE-eFluor 610-labeled anti-mouse IL-17A antibody (clone: 17B7; catalog number: 61-7177-82, Invitrogen)

for FACS study via a Thermo Fisher Attune NxT Analyzer or Intellicyt iQue Screener PLUS Analyzer in the Flow Cytometry Core Facility in the UNC School of Medicine.

Statistical Analysis

No statistical methods were used to pre-determine the sample size of the experiment. The sample sizes were based on similar published *in vitro* and *in vivo* studies.[24, 47] No collected experimental data was excluded for the quantitative analysis. Quantitative data were expressed as mean ± standard error of the mean (SEM). For *in vitro* data, statistical significnt between two control/experiment groups were assessed by two-way ANOVA with Tukey correction in the Graph Pad Prism 6 software pack. The analysis of variance of *in vivo* data was completed using two-tailed t-tests in the Graph Pad Prism 6 software pack. * $P < 0.05$ was considered statistically significant; n.s. $P > 0.05$ was considered statistically insignificant.

Supporting Figures

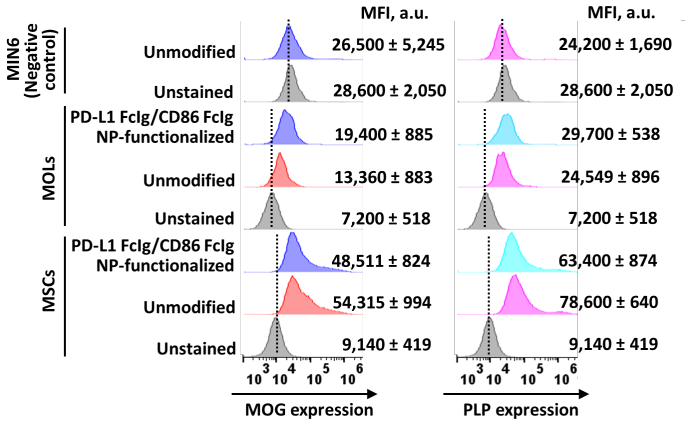

Figure S1. MSCs and MOLs express common myelin antigens. Representative FACS histograms of anti-MOG- and anti-PLP1-stained MSCs, MOLs, and MIN6 cells (insulinoma cells isolated C57BL/6 mice). Both anti-MOG and anti-PLP1 rabbit polyclonal antibodies were labeled *via* A488-labeled goat anti-rabbit IgG. The MIN6 cells were used for negative control.

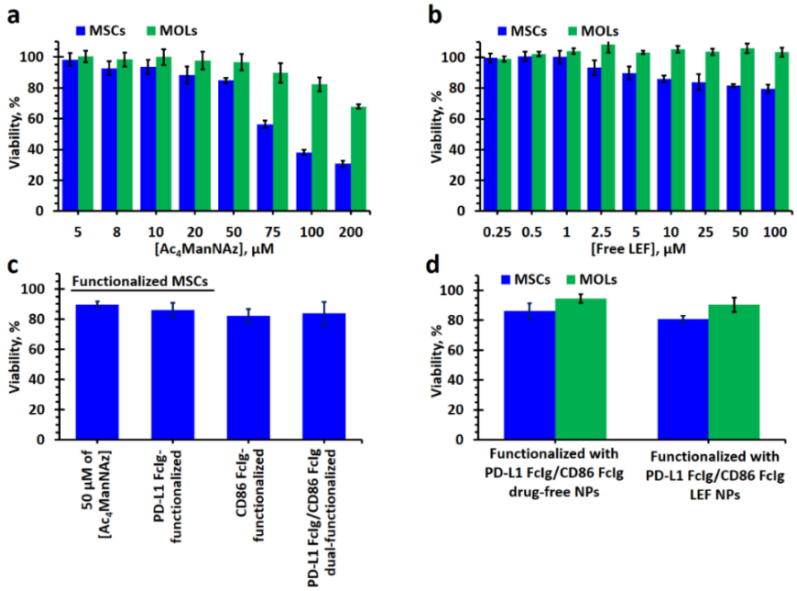

Figure S2. MSCs and MOLs remain viable after incubated with small-molecule Ac_4ManNAz, small-molecule LEF, and after bioconjugation. a) *In vitro* viabilities of MSCs and MOLs after incubated with different concentrations of small-molecule Ac_4ManNAz, as quantified by MTS assay. b) *In vitro* viabilities of MSCs and MOLs after incubated with different concentrations of small-molecule LEF, as quantified by MTS assay. Small-molecule LEF showed moderate *in vitro* toxicity against MSCs and insignificant toxicity against MOLs. This suggests LEF would not affect OLs (that already in the CNS) to repair the damaged myelin. c) Relative viabilities of different directly functionalized MSCs, as determined by MTS assay. d) Relative viabilities of drug-free and LEF-loaded PD-L1 FcIg/CD86 FcIg NP-functionalized MSCs and MOLs, as determined by MTS assay. (n = 8)

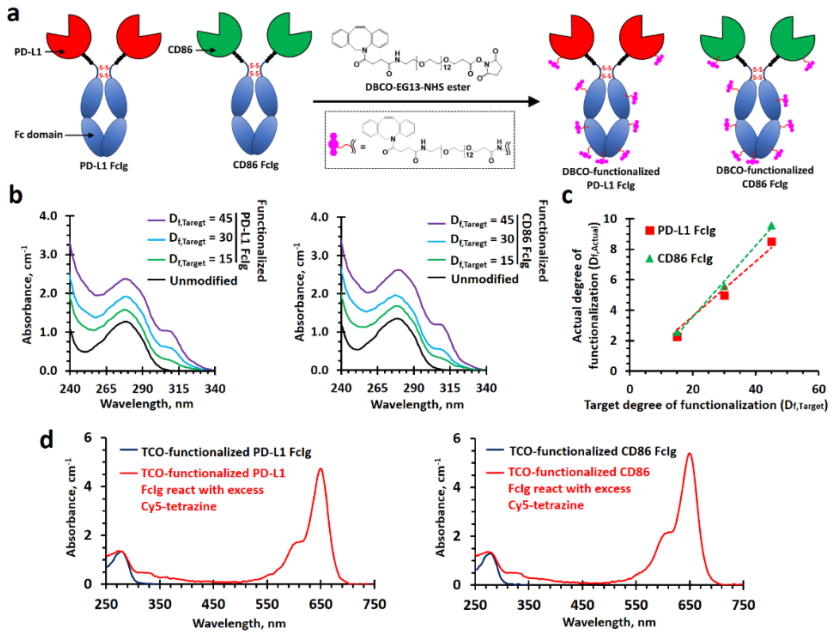

Figure S3. Characterization of DBCO-functionalized PD-L1 FcIg and DBCO-functionalized CD86 FcIg. a) The scheme illustrates covalent conjugation of DBCO-functionalized ethylene glycol (EG) to the PD-L1 and CD86 FcIg fusion proteins through amine-N-hydroxysuccinimide (NHS) ester coupling reaction at different target degree of functionalization ($D_{f,\,Target}$). b) UV-visible absorption spectra of different DBCO-functionalized PD-L1 FcIg and CD86 FcIg fusion proteins (1 mg/mL). c) The plot of the actual degree of functionalization of PD-L1 FcIg and CD86 FcIg. DBCO-functionalized PD-L1 FcIg (with 8 conjugated DBCO) and DBCO-functionalized CD86 FcIg (with 9 conjugated DBCO) prepared at a $D_{f,\,Target}$ of 45 were used for functionalization of MSCs and MOLs. d) UV-visible absorption spectra of TCO-functionalized PD-L1 FcIg and CD86 FcIg (1 mg/mL). Both TCO-functionalized fusion proteins were functionalized as with the DBCO-functionalized fusion proteins with a target degree of functionalization of 45. e) UV-visible absorption spectra of purified TCO-functionalized PD-L1 FcIg and CD86 FcIg after reacted with 5 molar equivalents of Cy5 tetrazine (probe) at 37 ˚C for 1 h (normalized to 1 mg/mL). The reactions were carried out at a protein concentration of 0.5 mg/mL in serum- and phenol red-free DMEM medium (the same fusion protein concentration that used in functionalization of MSCs). Unreactive dye and DMEM were removed *via* PD-10 desalting columns. Both functionalized fusion proteins contain less conjugated *active* TCO were removed *via* PD-10 desalting columns. Both functionalized fusion proteins contain less conjugated *active* TCO (an average of 2 *active* TCO molecule per fusion protein) than that functionalized with DBCO ligand because of trans-to-cis isomerization at the basic conjugation condition inactivated the TCO ligand and thiols in culture medium reacted with the conjugated TCO.

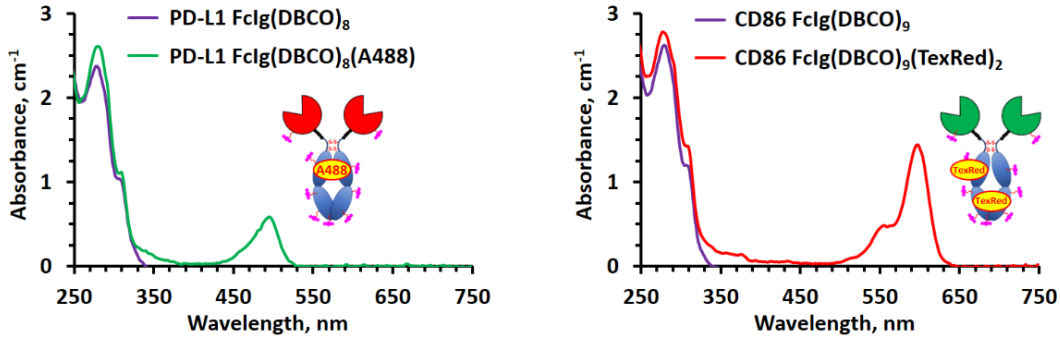

Figure S4. Characterization of A488-labeled DBCO-functionalized PD-L1 FcIg and Texas Red-labeled DBCO-functionalized CD86 FcIg. Representative UV-visible spectra of non-labeled DBCO-functionalized fusion PD-L1 FcIg, CD86 FcIg, A488-labeled DBCO-functionalized PD-L1 FcIg fusion protein, and Texas Red-labeled DBCO-functionalized PD-L1 FcIg fusion protein. It was calculated that the functionalized PD-L1 FcIg fusion protein contains an average of one conjugated A488 molecule. The functionalized CD86 FcIg fusion protein contains an average of two conjugated Texas Red molecules.

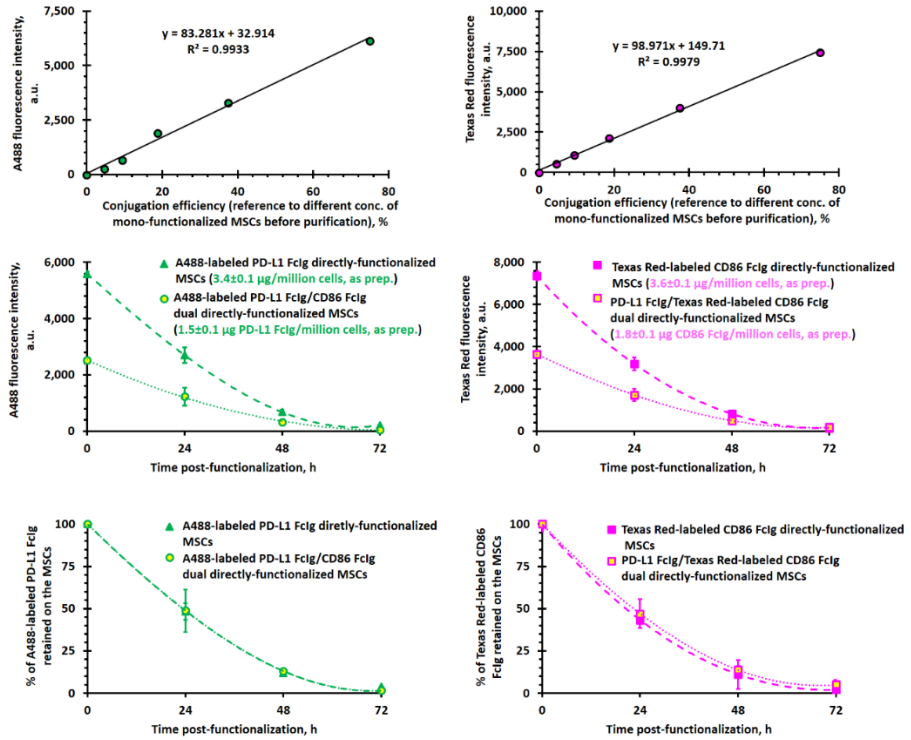

Figure S5. Covalently conjugated PD-L1 FcIg and CD86 FcIg gradually detached from mono- and dual-functionalized MSCs at the physiological conditions. Quantification of the detachment rate of A488-labeled PD-L1 FcIg and Texas Red-labeled CD86 FcIg from mono-and dual-functionalized MSCs at the physiological conditions *via* fluorescence spectroscopy. About half of the conjugated fusion proteins detached from the MSCs within 24 h after conjugation. (n = 8, cell seeding density = 10,000 cells per well.)

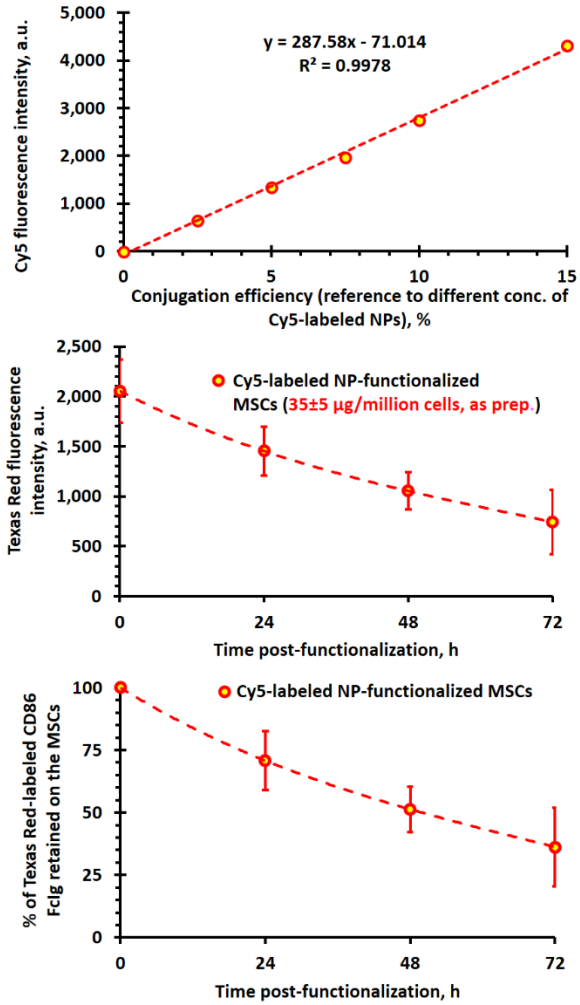

Figure S6. PD-L1 FcIg/CD86 FcIg Cy5-labeled NPs slowly detached from MSCs at the physiological conditions. Quantification of the detachment rate of PD-L1 FcIg/CD86 FcIg-conjugated Cy5-labeled NPs from MSCs at the physiological conditions *via* fluorescence spectroscopy. About half of the conjugated Cy5-labeled NPs retained on the MSCs 48 h after functionalization. (n = 8, cell seeding density = 10,000 cells per well.)

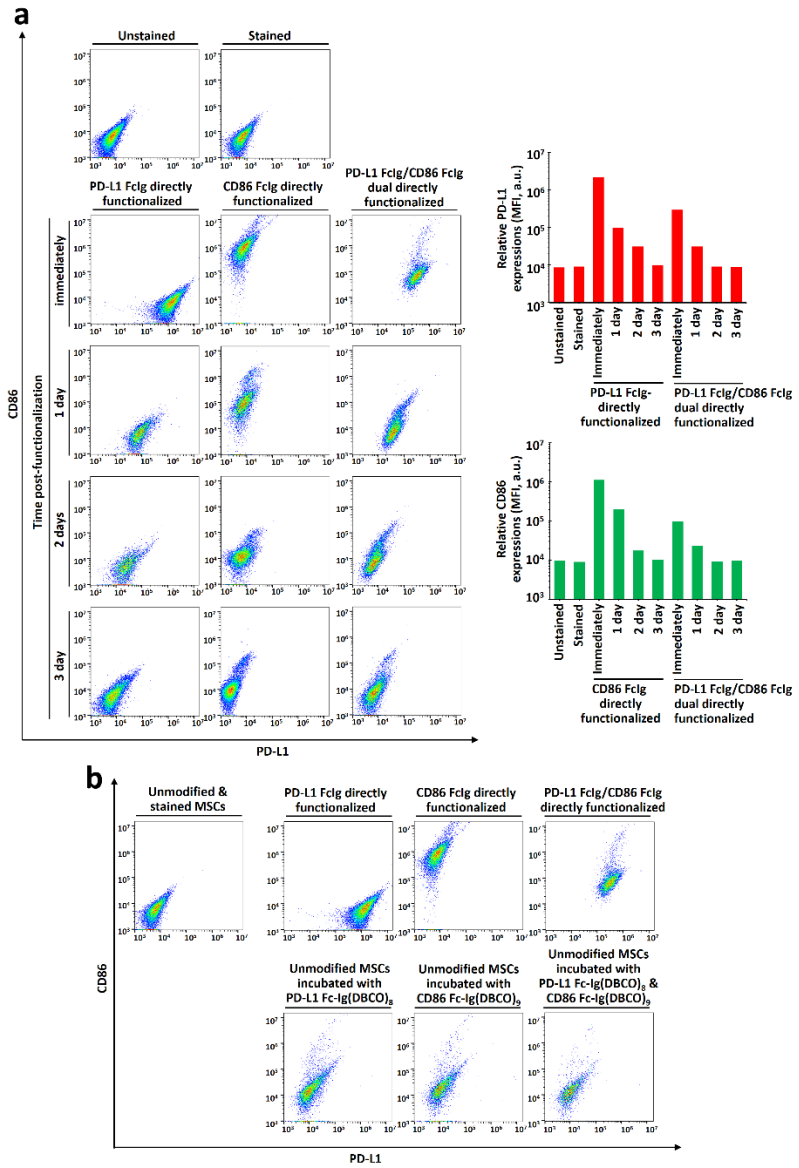

Figure S7. PD-L1 and CD86 expressions of PD-L1 FcIg/CD86 FcIg mono-/dual- directly functionalized MSCs gradually declined after functionalization. a) Representative FACS histograms show the PD-L1 and CD86 expressions of PD-L1 FcIg and CD86 FcIg mono- or dual- directly functionalized MSCs after stained with PE-labeled PD-L1 and A488-labeled CD86. The PD-L1 and CD86 expressions declined to the background level 3 days post-functionalization. (n = 3) b) Representative FACS histograms show the PD-L1 and CD86 expressions unmodified (azido-free) MSCs after incubated with PD-L1 FcIg and/or CD86 FcIg at physiological conditions for 1 h. The incubated cells were washed before stained with anti-PD-L1 and anti-CD86 antibodies for the FACS study. The FACS study confirmed that the bioconjugation process does not induce significant non-specific binding of FcIg fusion proteins.

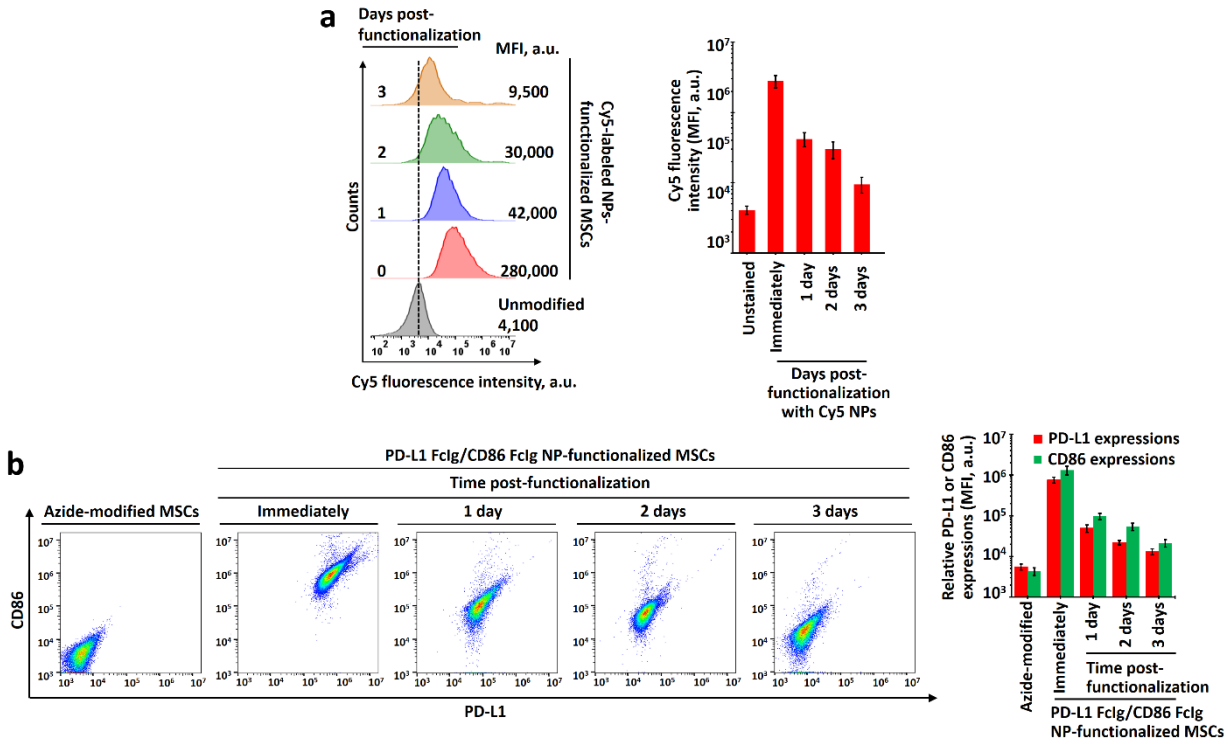

Figure S8. PD-L1 FcIg/CD86 FcIg NP slowly detached from the surface of azide-modified MSCs after functionalization. a) Representative FACS histograms show the Cy5 fluorescence intensities of PD-L1 FcIg/CD86 FcIg Cy5-labeled NP-functionalized MSCs recorded at different times after functionalization. b) Representative FACS histograms show the PD-L1 and CD86 expressions of PD-L1 FcIg and CD86 FcIg NP-functionalized MSCs after stained with PE-labeled PD-L1 and A488-labeled CD86. The PD-L1 and CD86 expressions slowly decline to the background level 3 days post-functionalization. (n = 3)

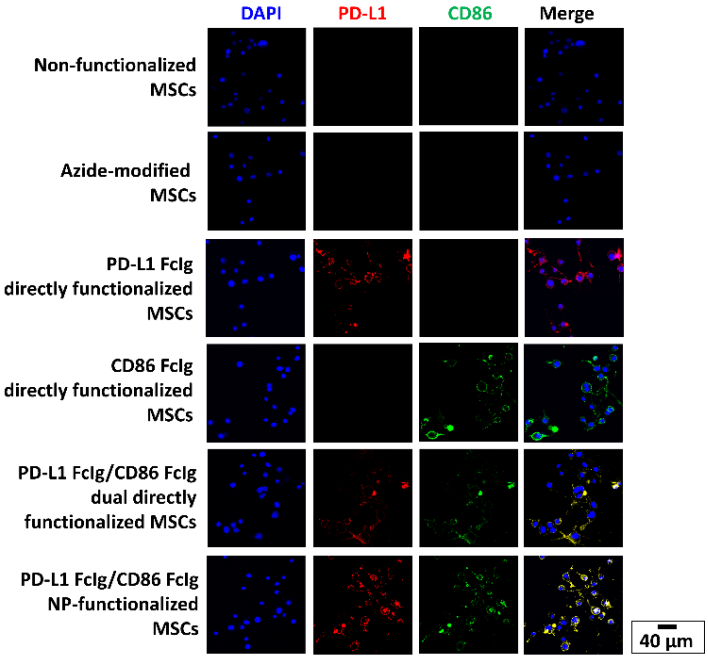

Figure S9. Successful conjugation of PD-L1 FcIg and/or CD86 FcIg onto the surface of azide-modified MSCs. Representative CLSM images of unmodified and the as-functionalized MSCs after stained with PE-labeled anti-PD-L1 and A488-labeled anti-CD86 antibodies.

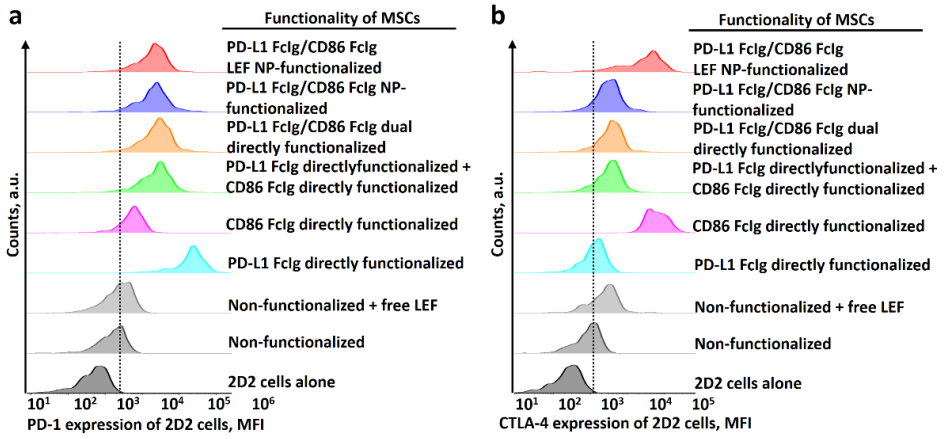

Figure S10. PD-L1- and CD86-bioengineered MSCs upregulate the PD1 and CTLA-4 expressions of the incubated 2D2 cells. a) Representative FACS histograms of A488-labeled anti-PD-1 stained 2D2 cells (MOG-specific $CD4^+$ cells) after incubated with different functionalized MSCs at an effector:target ratio (E/T) of 10:1 for 48 h. b) Representative FACS histograms of PE-labeled anti-CTLA-4 stained 2D2 cells (MOG-specific $CD4^+$ cells) after incubated with different functionalized MSCs at a E/T ratio of 10:1 for 48 h.

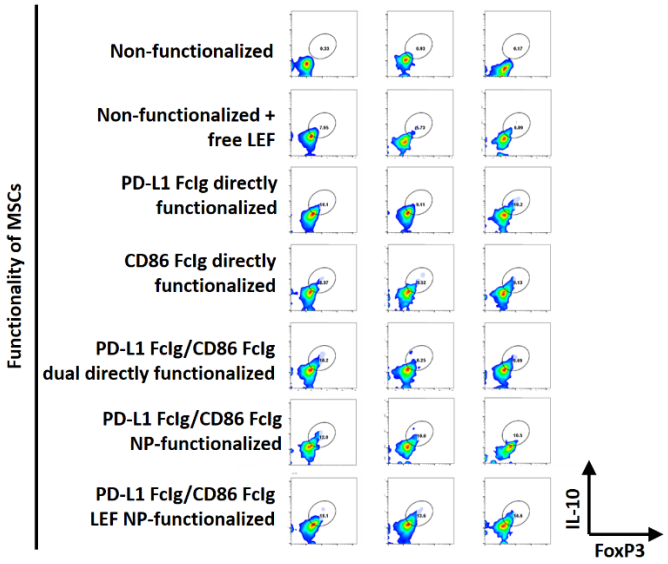

Figure S11. PD-L1-and CD86-bioengineered MSCs promote the development of antigen-specific IL10^{+} FoxP3^{+} T_{reg} cells. Representative two-dimensional FACS plots of A488-labeled anti-FoxP3- and PE-labeled anti-IL10- intracellular stained 2D2 cells after incubated with different functionalized MSCs at an E/T ratio of 10:1 for 3 days. The bioengineered MSCs promote the development of IL10^{+} and FoxP3^{+} T_{reg} cells. Cells were initially gated at CD3^{+} cells. (n = 3)

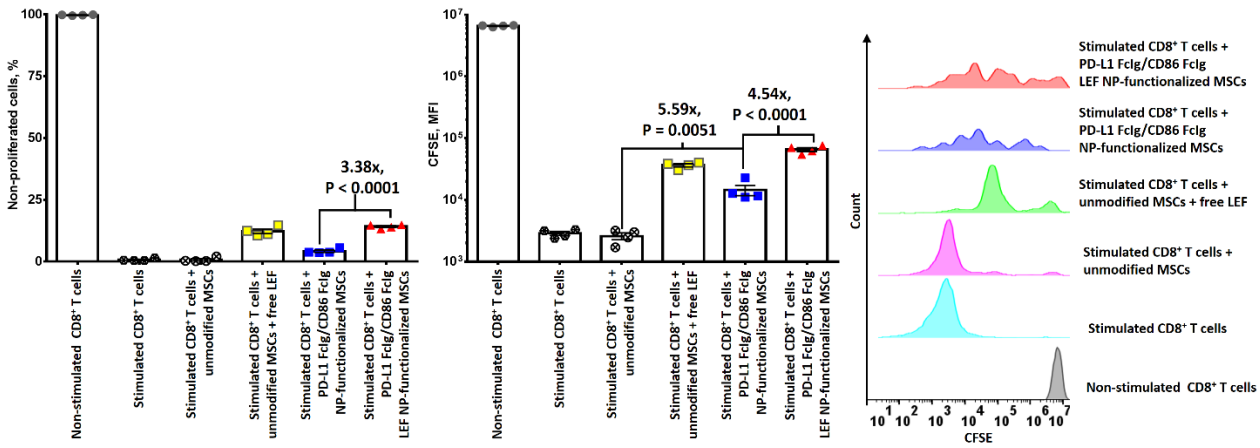

Figure S12. PD-L1 FcIg/CD86 FcIg NP-functionalized MSCs inhibit the proliferation of stimulated cytotoxic T cells in an antigen-non-specific behavior. CFSE-dilution assay of CFSE-labeled CD8^{+} T cells (isolated from wide-type C57BL/6 mice) after incubated with different functionalized MSCs at an E: T of 1:1 for 48 h. The cytotoxic T cells were cultured under stimulation conditions (i.e., in the presence of Dynabeads T Cell Activation beads at a 1:1 molar ratio). The proliferation of cytotoxic T cells was quantified *via* the FACS method. Cells were initially gated at CD8^{+} cells. (n = 4)

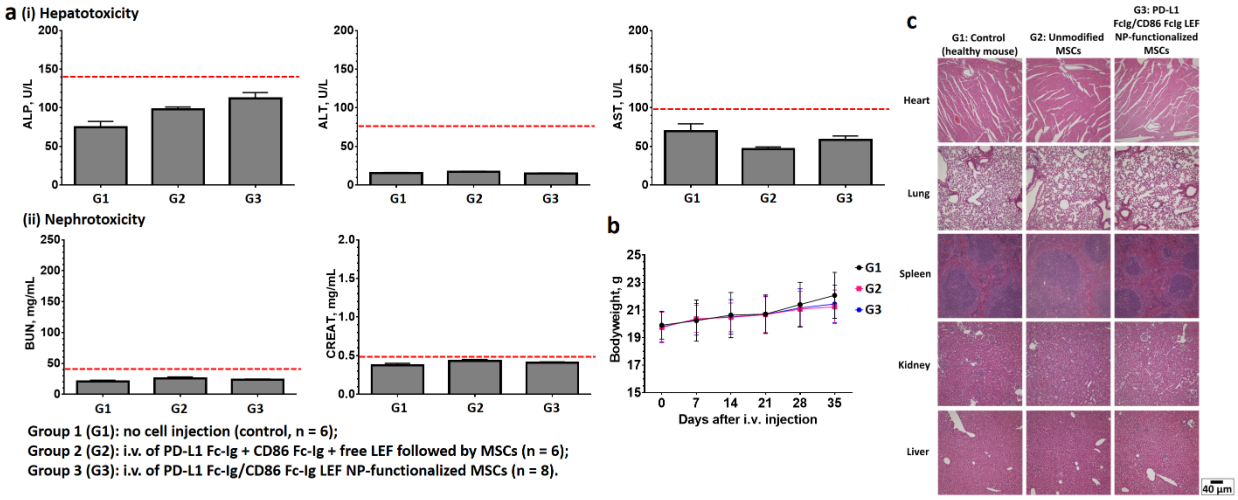

Figure S13. Intravenous administration of unmodified MSCs and PD-L1 FcIg/CD86 FcIg NP-functionalized MSCs did not cause long-term side effects. a) Clinical chemistry of blood samples collected from healthy untreated C57BL/6 mice (female, about 15 weeks old) and healthy C57BL/6 mice after i.v. administration of unmodified MSCs or PD-L1 FcIg/CD86 FcIg NP-functionalized MSCs (2×10^6 cells/mouse). The blood samples were collected 5 weeks post-administration of the MSCs. b) Bodyweight change of healthy C57BL/6 mice after i.v. administration of unmodified MSCs or PD-L1 FcIg/CD86 FcIg NP-functionalized MSCs (2×10^6 cells/mouse). The red dotted line represents the normal range of each blood chemistry parameter. c) Representative H&E-stained heart, lung, spleen, kidney, and liver session preserved from C57BL/6 mice 5 weeks after i.v. administration of MSCs or PD-L1 FcIg/CD86 FcIg NP-functionalized MSCs. (n = 6, excepted n = 8 for the experimental group i.v. administered with the PD-L1 FcIg/CD86 FcIg NP-functionalized MSCs.)

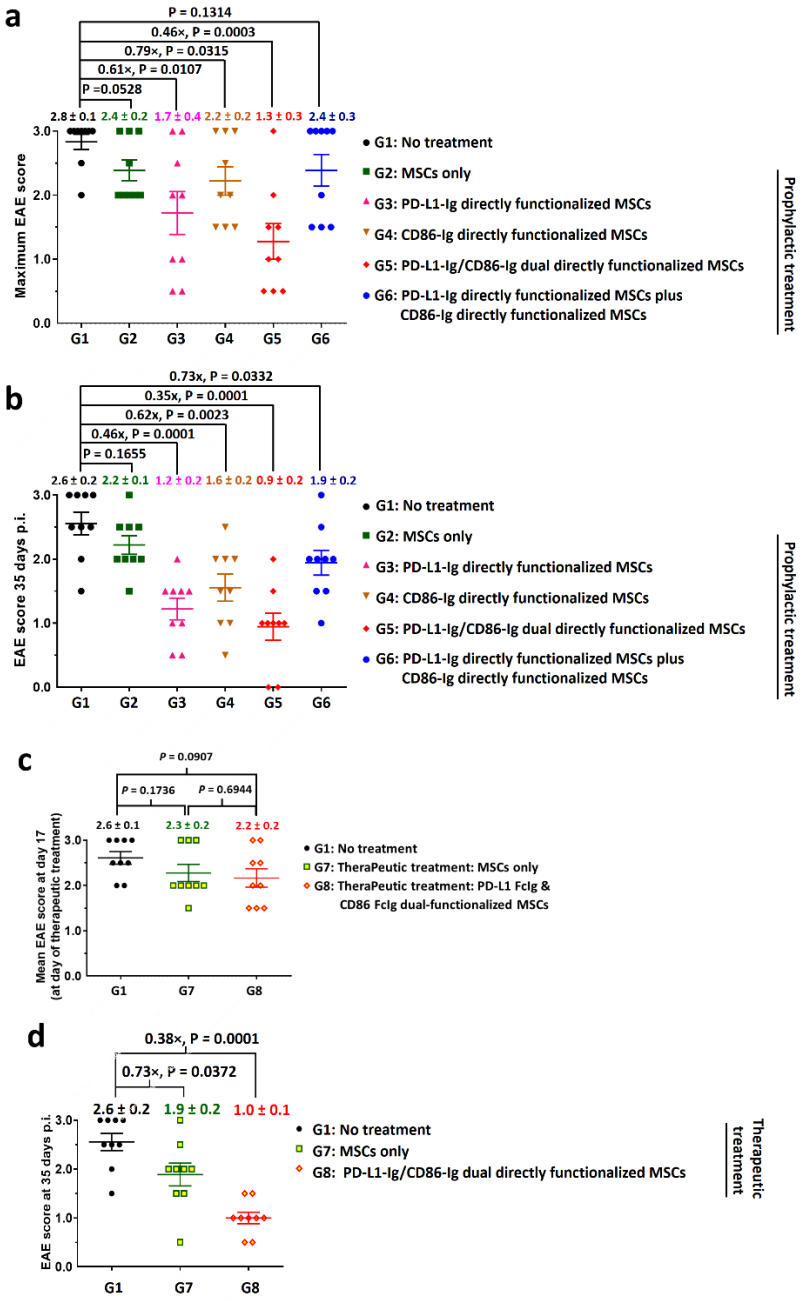

Figure S14. PD-L1 FcIg/CD86 FcIg directly functionalized MSCs suppress active MOG_{35-55}-induced EAE, prophylactically and therapeutically. a) Maximum EAE scores in mice after received prophylactic treatment (at 1-day p.i.) with unmodified or different directly functionalized MSCs (2×10^6 cells per mouse, *via* i.v. injection). b) EAE scores of MOG-induced EAE mice (at 35-days p.i.) after received prophylactic treatment (at 1-day p.i.) with unmodified or different directly functionalized MSCs. c) EAE scores of non-treatment group (G1) and therapeutic treatment groups (G7 and 8) 17 days post-immunization (before therapeutic treatment). The EAE scores of all three groups are statisitically similar, i.e. $P > 0.05$. d) EAE scores of MOG-induced EAE mice (at 35-days p.i.) after received therapeutic treatment (at 17-days p.i.) with unmodified and directly functionalized MSCs. (n = 9)

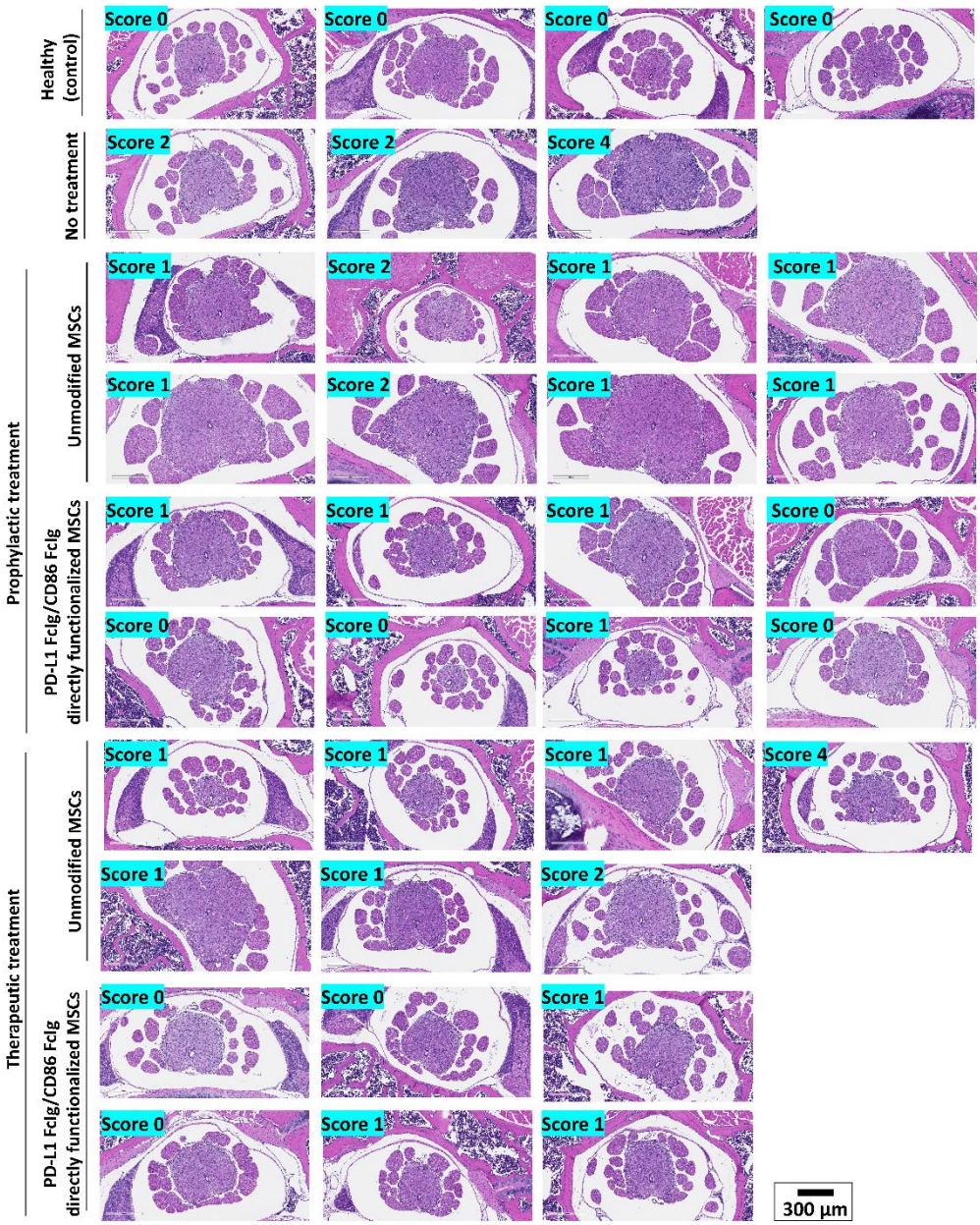

Figure S15. Drug-free and LEF-encapsulated PD-L1 FcIg/CD86 FcIg NP-functionalized MSCs effectively prevent and ameliorate active MOG_{35-55}-induced EAE by inhibiting spinal inflammation. Representative H&E-stained spinal cord cross-sections (and the corresponding inflammatory score) of healthy and EAE-inflicted mice after prophylactic and therapeutic treatment with drug-free and LEF-encapsulated PD-L1 FcIg/CD86 FcIg LEF NP-functionalized MSCs. Mice received prophylactic treatment on day 1 p.i., and therapeutic treatment on day 17 p.i. Spinal columns were preserved 36 or 37 days p.i.

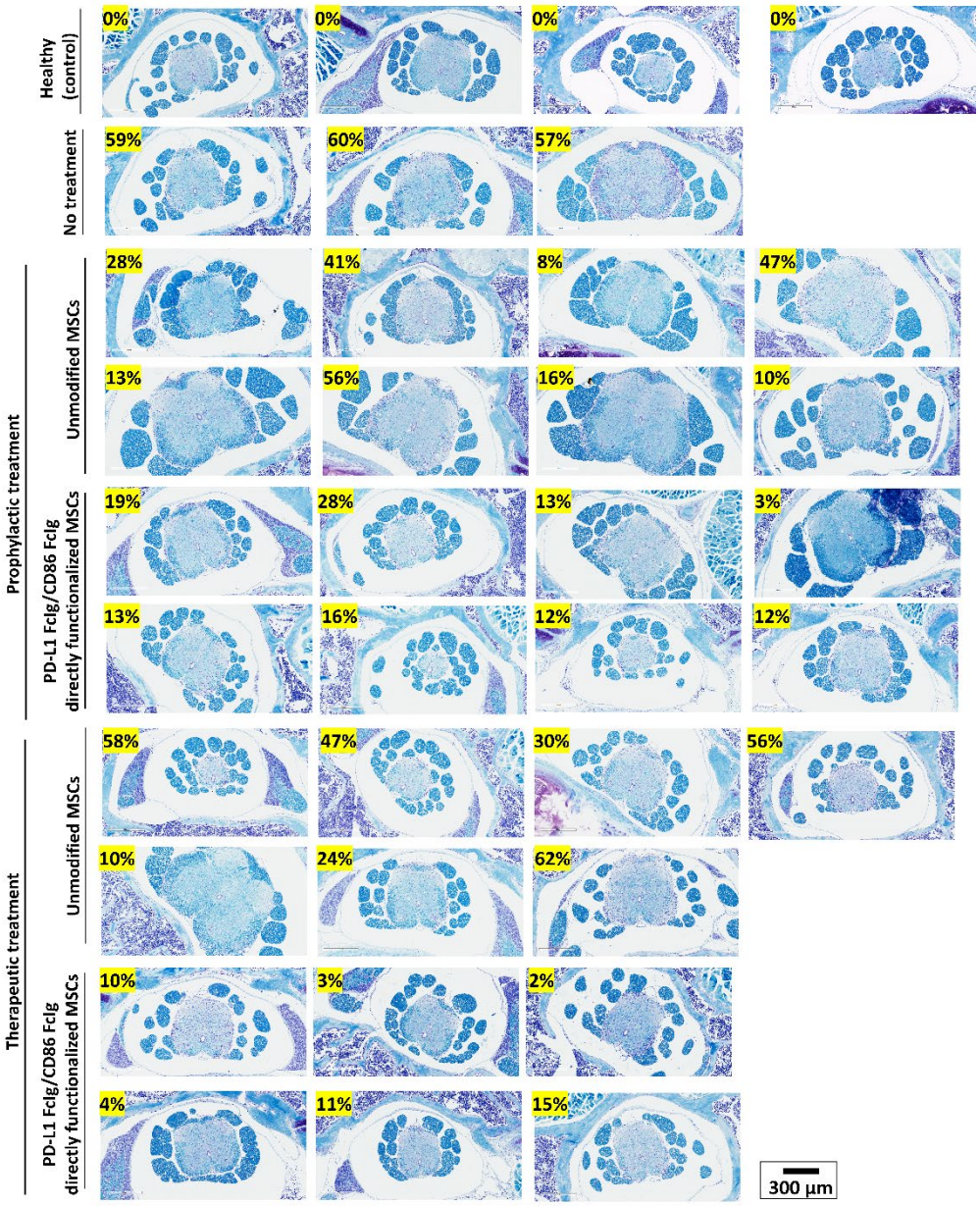

Figure S16. Drug-free and LEF-encapsulated PD-L1 FcIg/CD86 FcIg NP-functionalized MSCs effectively prevent and ameliorate active MOG_{35-55}-induced EAE by preventing demyelination. Representative ~~LEF~~ LFB-stained spinal cord cross-sections (and the corresponding inflammatory score) of healthy and EAE-inflicted mice after prophylactic and therapeutic treatment with drug-free and LEF-encapsulated PD-L1 FcIg/CD86 FcIg LEF NP-functionalized MSCs. Mice received prophylactic treatment on day 1 p.i., and therapeutic treatment on day 17 p.i. Spinal columns were preserved day 36 or 37 p.i.

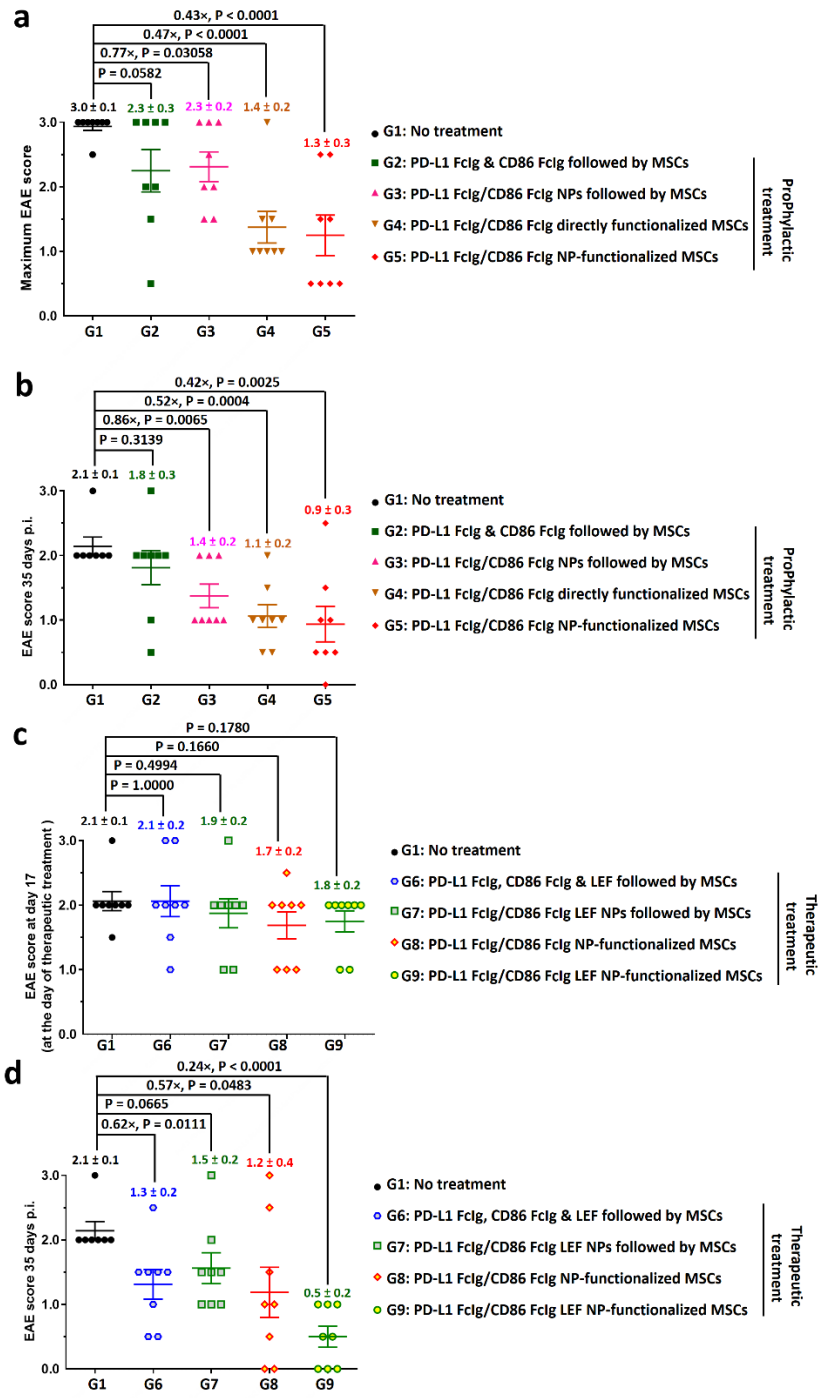

Figure S17. PD-L1 FcIg/CD86 FcIg LEF NP-functionalized MSCs suppress active MOG_{35-55}-induced EAE, prophylactically and therapeutically. a) Maximum EAE scores in mice after received prophylactic treatment (at 1-day p.i.) with unmodified or different NP functionalized MSCs (2×10^6 cells per mouse, *via* i.v. injection). b) EAE scores of MOG-induced EAE mice (at 35-days p.i.) after received prophylactic treatment (at 1-day p.i.) with unmodified or different NP functionalized MSCs. c) EAE scores of non-treatment group (G1) and therapeutic treatment groups (G6-G9 and 8) 17 days post-immunization (before therapeutic treatment). The EAE scores of all three groups are statisitically similar, i.e. $P > 0.05$. d) EAE scores of MOG-induced EAE mice (at 35 days p.i.) after received therapeutic treatment (at 17-days p.i.) with unmodified or different NP functionalized MSCs. (n = 8 mice per group; one non-treatment group mouse was found dead 28 days p.i.)

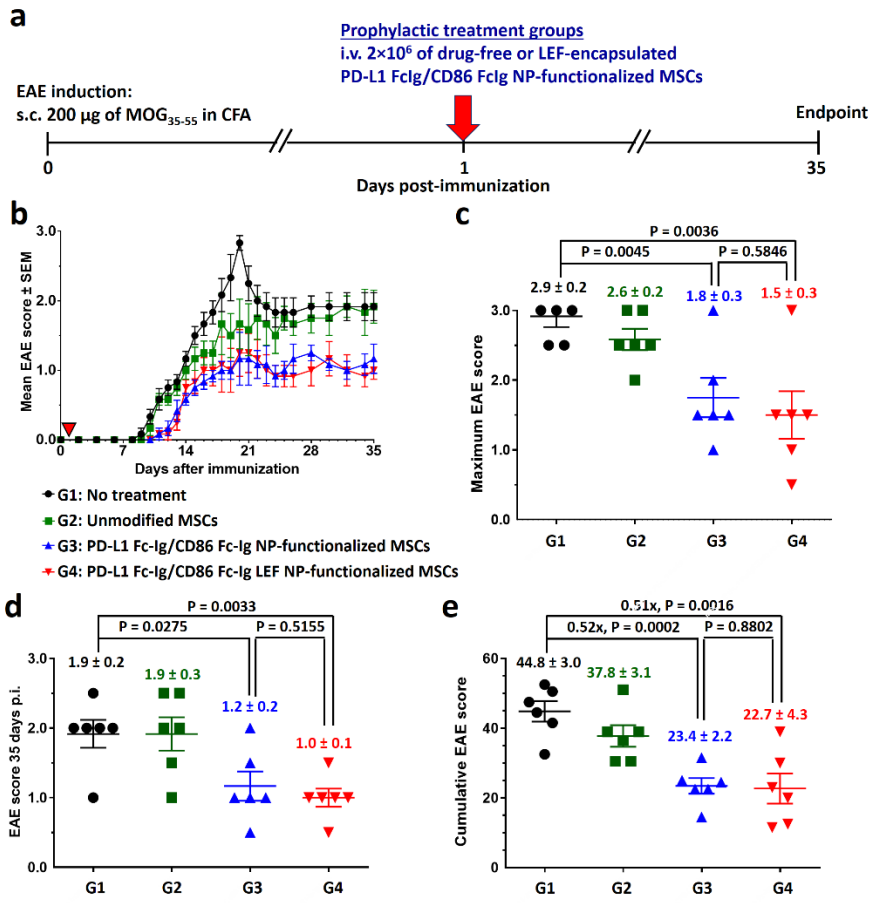

Figure S18. Drug-free and LEF-encapsulated PD-L1 FcIg/CD86 FcIg NP-functionalized MSCs are equally effective in preventing the development of severe EAE symptoms in the MOG_{35-55}-induced EAE model. a) Prophylactic treatment schedule. Drug-free and LEF-encapsulated PD-L1 FcIg/CD86 FcIg NP-functionalized MSCs (2×10^6 cells per mouse) were i.v. administrated 24 h p.i. b) Time-dependent EAE scores after prophylactic treatment with drug-free and LEF-encapsulated PD-L1 FcIg/CD86 FcIg NP-functionalized MSCs. c, Maximum EAE after different prophylactic treatments. d) EAE score recorded at day 35 p.i. after different prophylactic treatments. e) Cumulative EAE score (up to 35-days p.i.) after different prophylactic treatments. (n = 6)

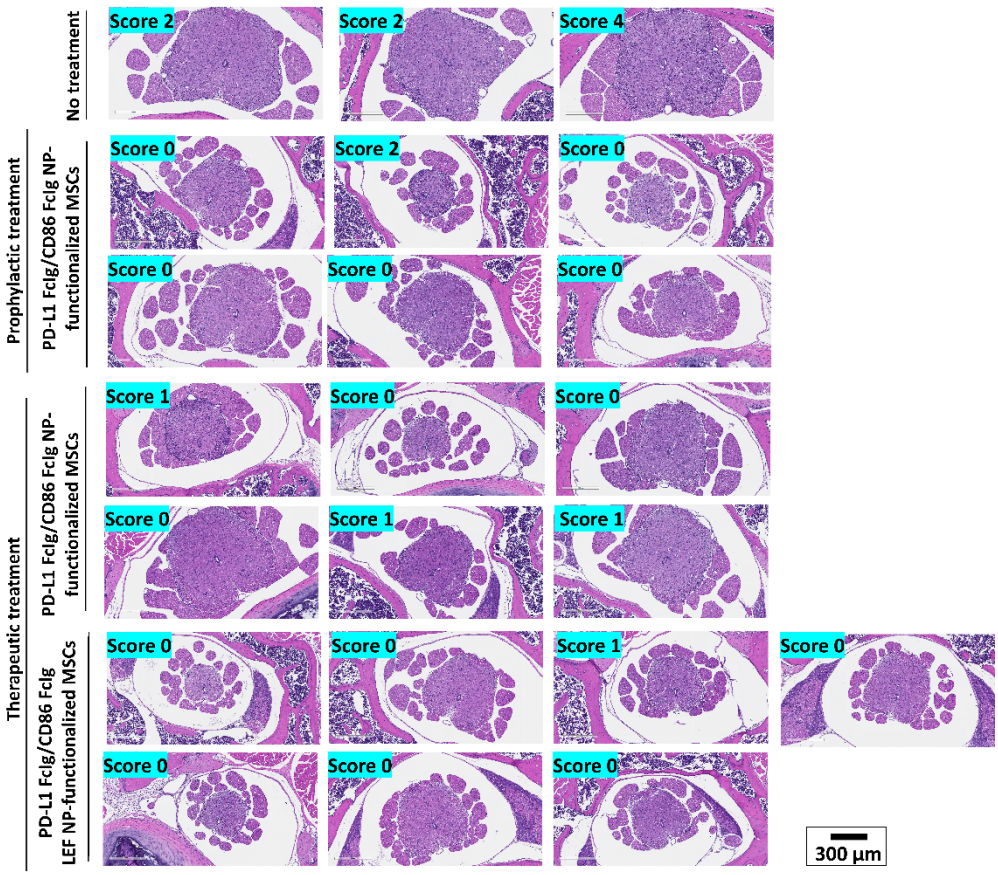

Figure S19. Drug-free and LEF-encapsulated PD-L1 FcIg/CD86 FcIg NP-functionalized MSCs effectively prevent and ameliorate active MOG_{35-55}-induced EAE by inhibiting spinal inflammation. Representative H&E-stained spinal cord cross-sections (and the corresponding inflammatory score) of healthy and EAE-inflicted mice after prophylactic and therapeutic treatment with drug-free and LEF-encapsulated PD-L1 FcIg/CD86 FcIg LEF NP-functionalized MSCs. Mice received prophylactic treatment on day 1 p.i., and therapeutic treatment on day 17 p.i. Spinal columns were preserved 36 or 37 days p.i.

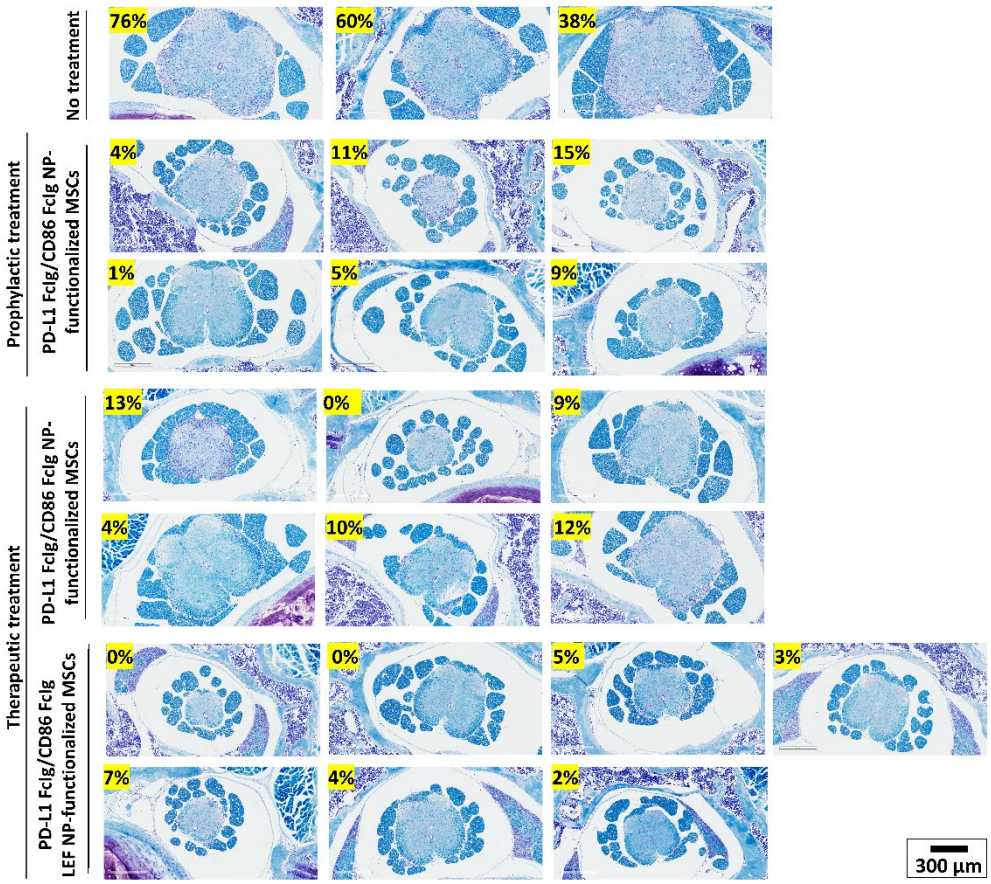

Figure S20. Drug-free and LEF-encapsulated PD-L1 FcIg/CD86 FcIg NP-functionalized MSCs effectively prevent and ameliorate active MOG_{35-55}-induced EAE by preventing demyelination. Representative ~~LEF~~ LFB-stained spinal cord cross-sections (and the corresponding inflammatory score) of healthy and EAE-inflicted mice after prophylactic and therapeutic treatment with drug-free and LEF-encapsulated PD-L1 FcIg/CD86 FcIg LEF NP-functionalized MSCs. Mice received prophylactic treatment on day 1 p.i., and therapeutic treatment on day 17 p.i. Spinal columns were preserved day 36 or 37 p.i.

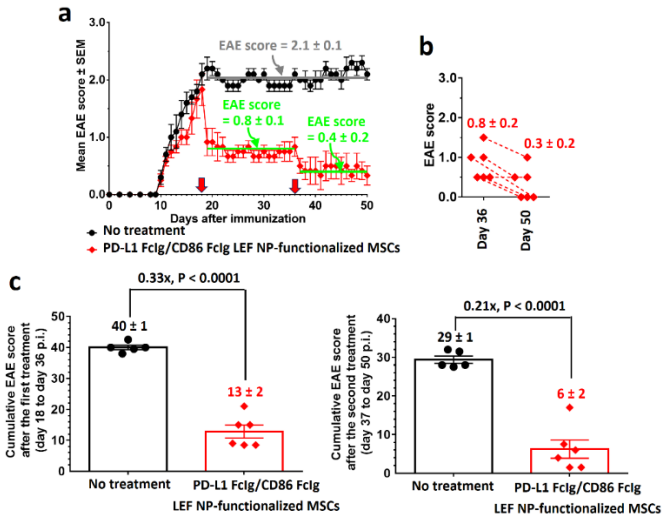

Figure S21. A booster dose of therapeutic treatment with PD-L1 FcIg/CD86 FcIg LEF NP-functionalized MSCs is more effective in suppressing active MOG_{35-55}-induced EAE. a) Time-dependent EAE score after therapeutic treatments (at day 18 and 36 p.i.) with PD-L1 FcIg/CD86 FcIg LEF NP-functionalized MSCs (2×10^6 cells per mouse). b) EAE scores were recorded at day 35 (before second treatment) and day 50 p.i. (study endpoint). c) Cumulative EAE score of non-treatment and therapeutic treatment groups recorded between day 18 and 36 p.i. after the first treatment. d) Cumulative EAE score of non-treatment and therapeutic treatment groups recorded between day 37 and 50 p.i. after the second treatment. (n = 6. The mice reported in this study were identical to the non-treatment group and therapeutic treatment group (without T_{reg} cell depletion) mice reported in the mechanistic study (statistical analysis ended on day 28 p.i.).)

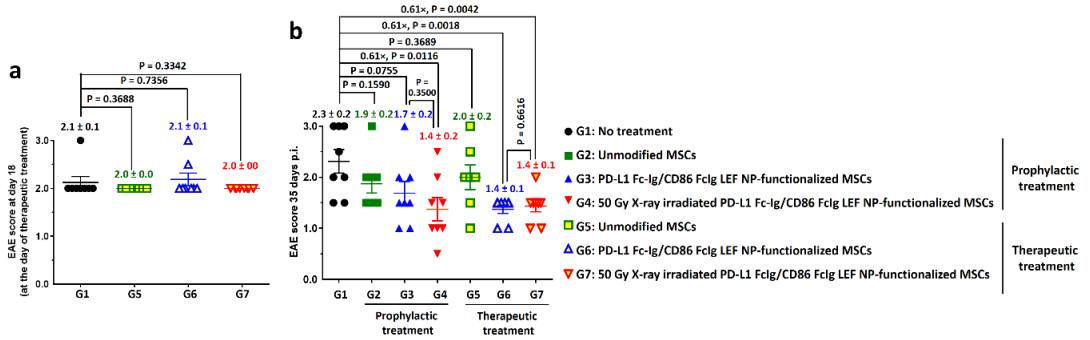

Figure S22. PD-L1 FcIg/CD86 FcIg LEF NP-functionalized MSCs suppress active $PLP_{178-191}$-induced EAE, prophylactically and therapeutically. a) EAE scores of non-treatment group (G1) and therapeutic treatment groups (G5-G7) 18 days post-immunization (before therapeutic treatment). The EAE scores of all three groups are statisitically similar, i.e. $P > 0.05$. b) EAE scores of $PLP_{178-191}$-induced EAE mice (recorded at 35-days p.i.) after received prophylactic treatment (at 1-day p.i.) or therapeutic treatment (at 18-days p.i.) with unmodified or different NP functionalized MSCs. (n = 8 mice per group, except n = 7 for the therapeutic treatment group with unmodified MSCs.)

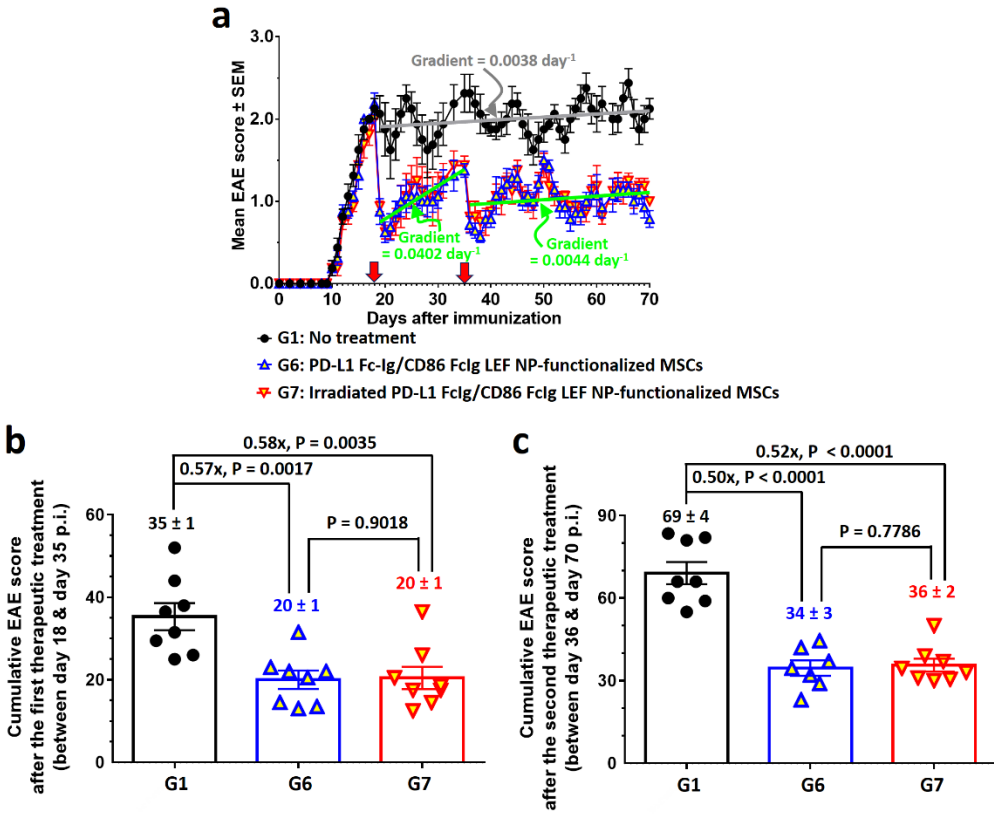

Figure S23. A second dose of therapeutic treatment with PD-L1 FcIg/CD86 FcIg LEF NP-functionalized MSCs effectively suppresses active $PLP_{178-191}$-induced EAE. a) Time-dependent EAE score after therapeutic treatments (at day 18 and 35 p.i.) with PD-L1 FcIg/CD86 FcIg LEF NP-functionalized MSCs (2×10^6 cells per mouse). The gradient of the plot represents the progression of the disease. Without any treatment, the progression rate was 0.0038 day^{-1}. The disease proregression rate was 0.0402 day^{-1} after the first therapeutic treatment. The disease progression rate dropped to 0.0044 day^{-1} after the second therapeutic treatment. b) Cumulative EAE score of non-treatment and therapeutic treatment group EAE-inflicted mice recorded between day 18 and 35 p.i. after the first treatment. c) Cumulative EAE score of non-treatment and therapeutic treatment group EAE-inflicted mice recorded between day 35 and 70 p.i. after the second treatment. (n = 8; one mouse in the therapeutic treatment Group 6 was found dead at day 37 p.i. (1 day after the second treatment).)

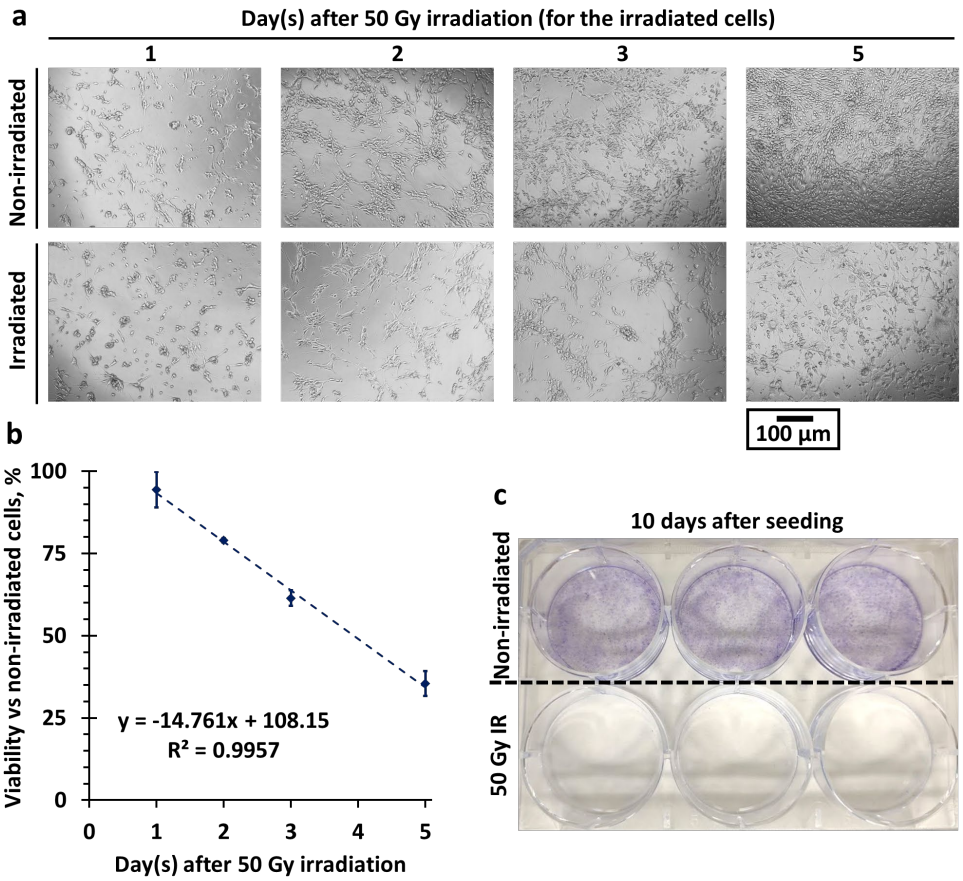

Figure S24. 50 Gy X-ray irradiation kills PD-L1 FcIg/CD86 FcIg LEF NP-functionalized MSCs. a) Time-dependent optical microscopy images of non-irradiated and 50 Gy X-ray-irradiated PD-L1 FcIg/CD86 FcIg LEF NP-functionalized MSCs. b) Relative viabilities of 50 Gy X-ray-irradiated PD-L1 FcIg/CD86 FcIg LEF NP-functionalized MSCs at different times after irradiation. (n = 8) c) Digital photograph of non-irradiated and 50 Gy X-ray-irradiated PD-L1 FcIg/CD86 FcIg LEF NP-functionalized MSCs after cultured at physiological conditions for 10 days. Colonies were stained by 1% crystal violet.

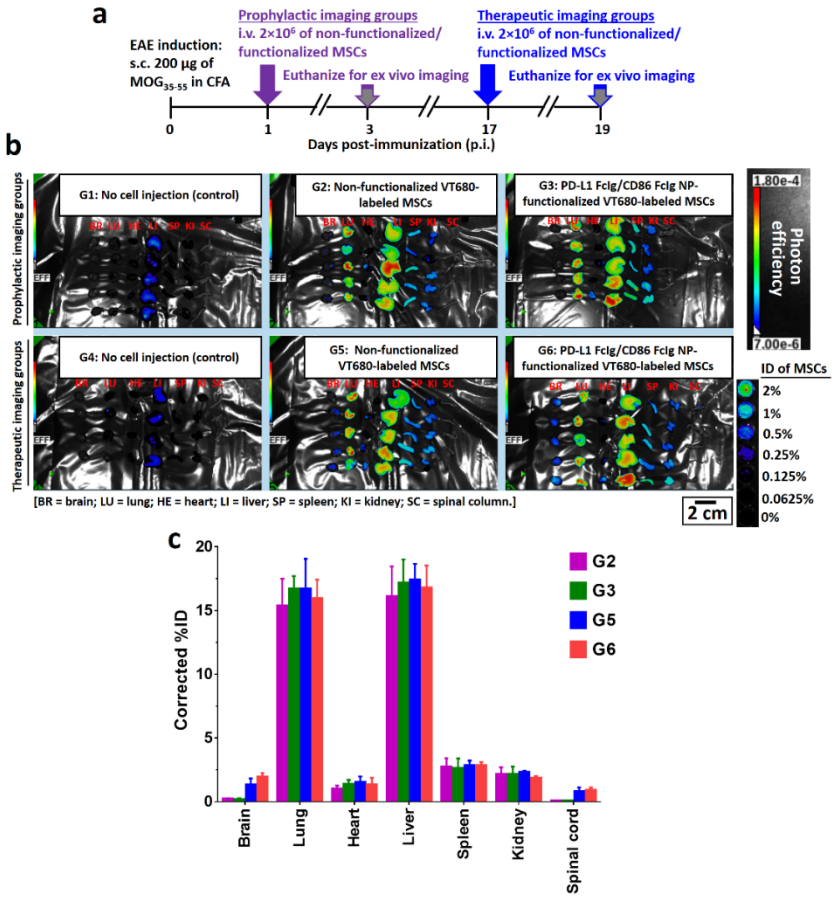

Figure S25. Biodistribution of i.v. administered non-functionalized and PD-L1 FcIg/CD86 FcIg NP-functionalized VT680-labeled MSCs in MOG_{35-55}-induced EAE mice. a) *Ex vivo* imaging schedules. EAE-inflicted mice were euthanized 48 h after i.v. administration of different VT680-labeled MSCs, either in a prophylactic study (at day 3) or therapeutic study (at day 19). b) *Ex vivo* fluorescent images of the brain (BR), lung (LU), heart (HE), liver (LI), spleen (SP), kidney (KI), and spinal cord (SC) preserved from non-treatment and different treatment group mice. c) Biodistribution of i.v. administered VT680-labeled MSCs. (n = 5)

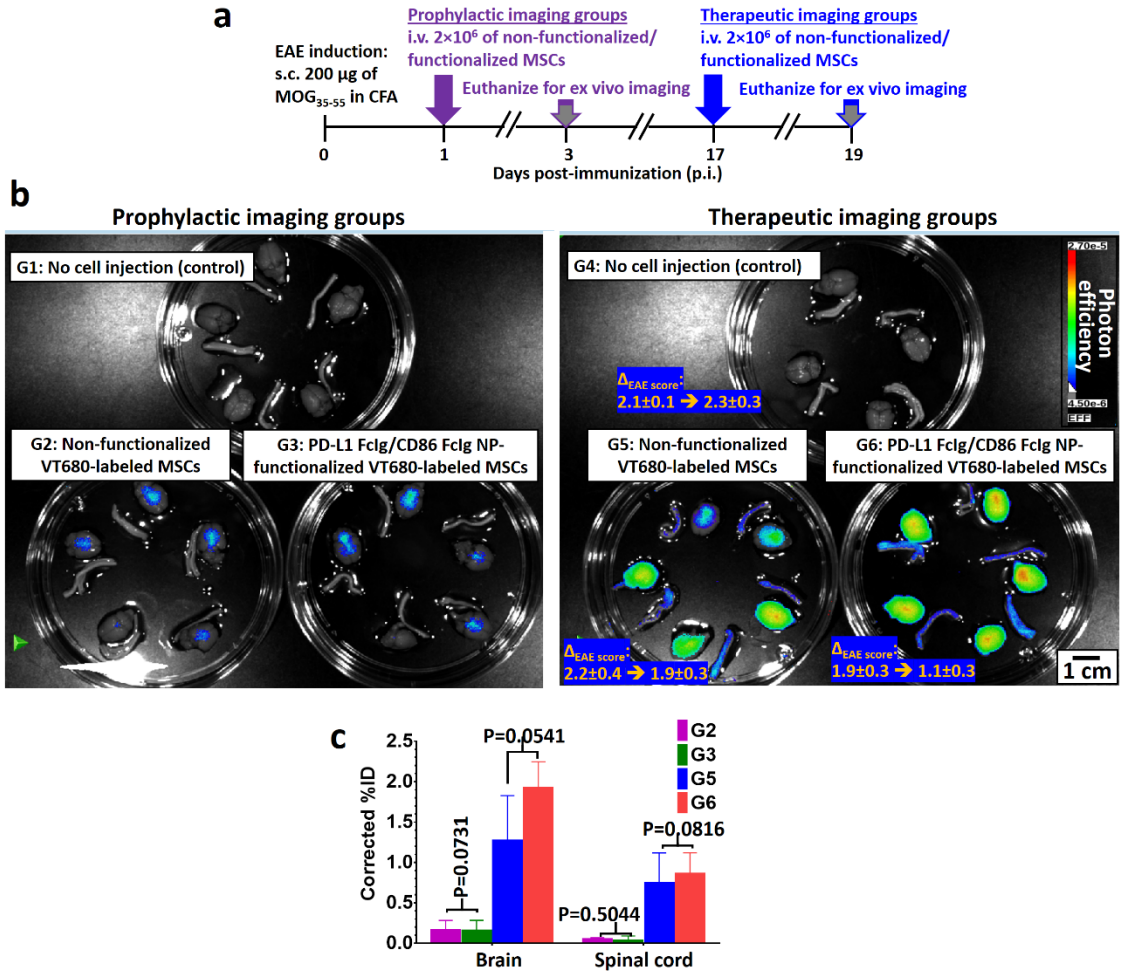

Figure S26. Biodistribution of i.v. administered non-functionalized and PD-L1 FcIg/CD86 FcIg NP-functionalized VT680-labeled MSCs in MOG_{35-55}-induced EAE mice. a) *Ex vivo* imaging schedules. EAE-inflicted mice were euthanized 48 h after i.v. administration of different VT680-labeled MSCs, either in a prophylactic study (at day 3) or therapeutic study (at day 19). b) *Ex vivo* fluorescent images of the brain (BR) and spinal cord (SC) preserved from non-treatment and different treatment group mice. c) Biodistribution of i.v. administered VT680-labeled MSCs. (n = 5)

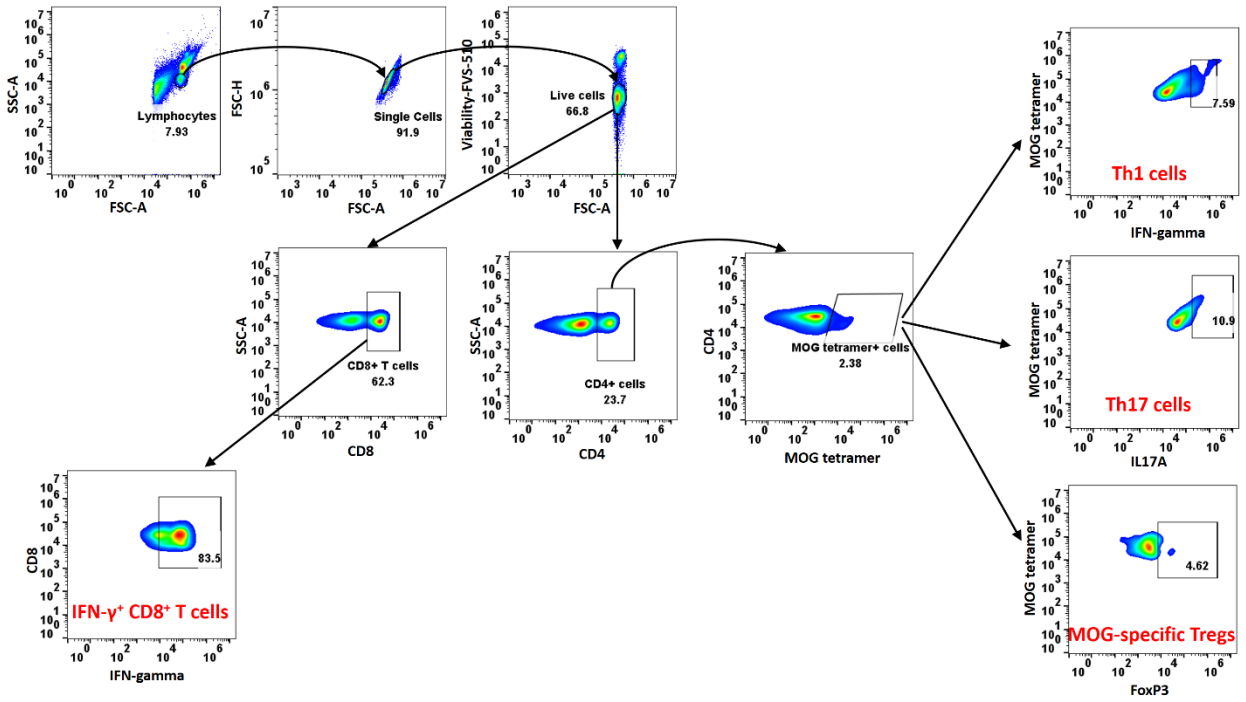

Figure S27. Representative FACS gating strategy for analyzing autoreactive $CD8^+$ T cell and different MOG-specific $CD4^+$ T cell populations in the spinal cord and spleen. Diagram summarizes the gating strategy for analysis the IFN-γ^+ $CD8^+$ T cells (autoreactive cytotoxic T cells), MOG-specific pathogenic T_h1 (MOG^+ IFN-γ^+ $CD4^+$) and T_h17 (MOG^+ $IL17A^+$ $CD4^+$) cells, and suppressive T_{reg} cells (MOG^+ $FoxP3^+$ $CD4^+$) in the isolated spinal lymphocytes. An identical gating strategy was used to analyze MOG-specific T_{h1} (MOG^+ T-bet^+ $CD4^+$), T_h17 (MOG^+ RORγt^+ $CD4^+$), and T_{reg} cells (MOG^+ $FoxP3^+$ $CD4^+$) in the isolated splenic lymphocytes.

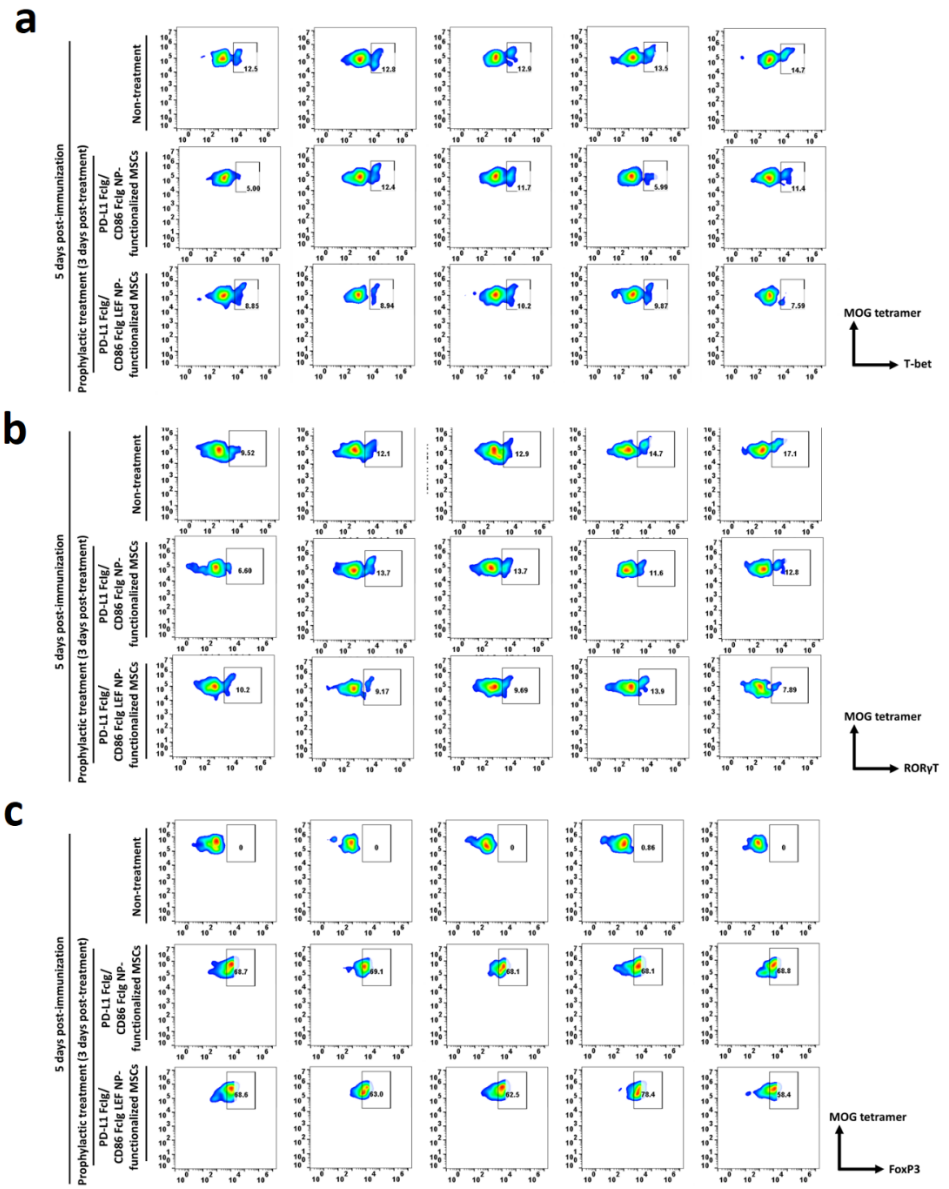

Figure S28. Drug-free and LEF-encapsulated PD-L1 FcIg/CD86 FcIg NP-functionalized MSCs are equally effective to induce the development of splenic MOG-specific T_{reg} cells to prevent the development of severe EAE symptoms. a) Two-dimensional FACS density plots showing the population of pathogenic MOG^+ $T\text{-}bet^+$ helper T cells (T_h1 cells) in the spleen 3 days after different therapeutic treatments. b) Two-dimensional FACS density plots showing the population of pathogenic MOG^+ $ROR\gamma t^+$ helper T cells (T_h17 cells) in the spleen 3 days after different therapeutic treatments. c) Two-dimensional FACS density plots showing the population of suppressive MOG^+ $FoxP3^+$ helper T cells (T_{reg} cells) in the spleen 3 days after different therapeutic treatments.

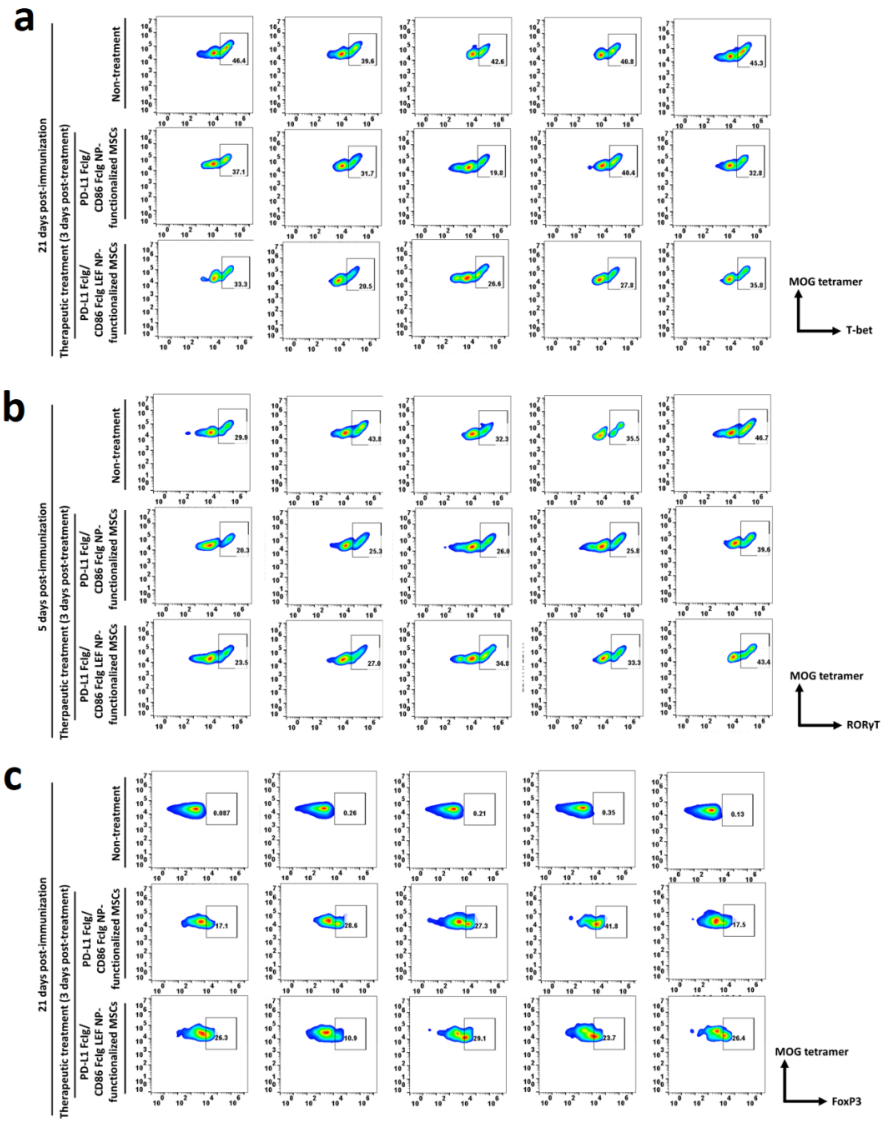

Figure S29. Drug-free and LEF-encapsulated PD-L1 FcIg/CD86 FcIg NP-functionalized MSCs are equally effective to induce the development of splenic MOG-specific T_{reg} cells to ameliorate severe EAE symptoms. a) Two-dimensional FACS density plots showing the population of pathogenic MOG^+ $T\text{-}bet^+$ helper T cells (T_h1 cells) in the spleen 3 days after different therapeutic treatments. b) Two-dimensional FACS density plots showing the population of pathogenic MOG^+ $ROR\gamma t^+$ helper T cells (T_h17 cells) in the spleen 3 days after different therapeutic treatments. c) Two-dimensional FACS density plots showing the population of suppressive MOG^+ $FoxP3^+$ helper T cells (T_{reg} s) in the spleen 3 days after different therapeutic treatments.

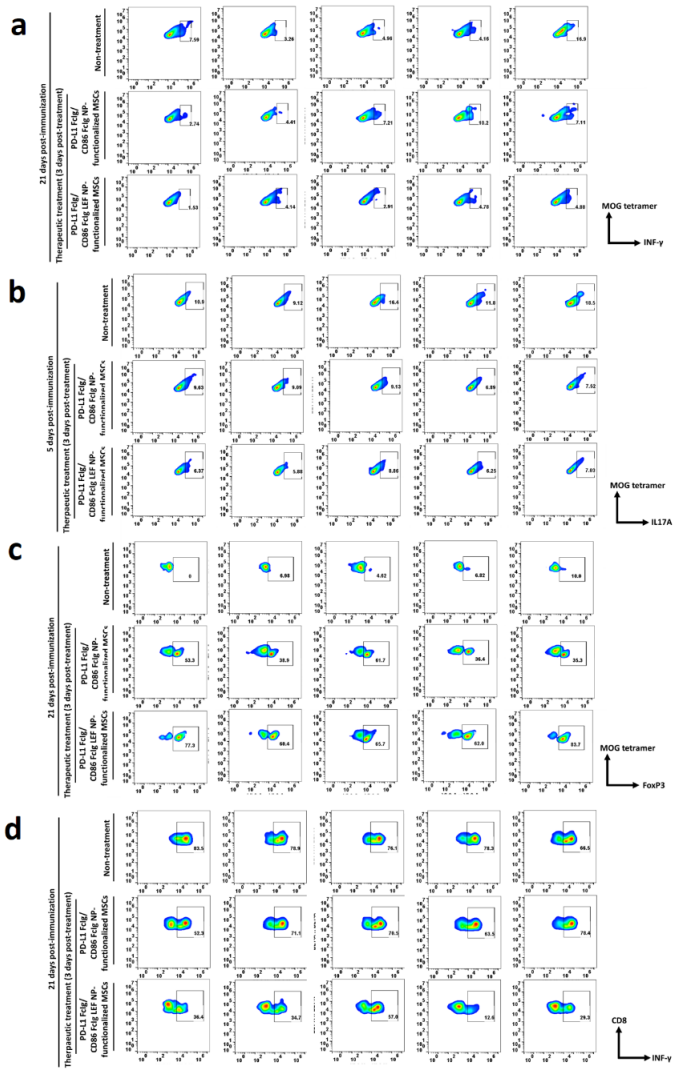

Figure S30. LEF-encapsulated PD-L1 FcIg/CD86 FcIg LEF NP-functionalized MSCs are more effective than drug-free PD-L1 FcIg/CD86 FcIg NP-functionalized MSCs to inhibit autoreactive cytotoxic T cells in the spinal cord and induce the development of spinal MOG-specific T_{reg} cells to ameliorate EAE symptoms. a) Two-dimensional FACS density plots showing the population of pathogenic MOG^+ $INF\text{-}\gamma^+$ helper T cells (T_h1 cells) in the spinal cord 3 days after different therapeutic treatments. b) Two-dimensional FACS density plots showing the population of pathogenic MOG^+ $IL17A^+$ helper T cells (T_h17 cells) in the spinal cord 3 days after different therapeutic treatments. c) Two-dimensional FACS density plots showing the population of suppressive MOG^+ $FoxP3^+$ helper T cells (T_{reg} cells) in the spinal cord 3 days after different therapeutic treatments. d) Two-dimensional FACS density plots showing the population of autoreactive $INF\text{-}\gamma^+$ cytotoxic T cells in the spinal cord 3 days after different therapeutic treatments.

Figure S31. Drug-free and LEF-encapsulated PD-L1 FcIg/CD86 FcIg NP-functionalized MSCs induced the development of suppressive T_{reg} cells long after the prophylactic and therapeutic treatments. Two-dimensional FACS density plots showing the population of suppressive MOG^{+} $FoxP3^{+}$ T_{reg} cells in the spleen 38 days p.i. after different prophylactic and therapeutic treatments.